Bachelor Thesis

Submitted for the degree of Bachelor of Science

Variability of the active layer freeze-back onset and duration in permafrost soil (Lena Delta, Siberia)

Submitted by:

Maybrit Pia Goldau

Supervisors:

Prof. Dr. Julia Boike

Dr. Inge Grünberg

Submitted at:

Department of Geography, Humboldt University of Berlin

10 July 2023

Abstract

Global climate change influences the soil temperature and active layer freeze-thaw processes in Arctic permafrost soils. Increasing permafrost temperatures have been extensively studied, but changes in seasonal freeze-thaw processes have often been less regarded. This work aimed to examine the variability of the active layer freeze-back onset and duration at the Arctic research site on Samoylov Island at the Lena River Delta in northeastern Siberia. Samoylov is underlain by continuous permafrost and characterized by a polygonal tundra landscape. I analyzed soil temperature data from 2014 to 2020 with respect to the polygon's microtopography. I estimated the timing of freeze-back at different depths in both the elevated rim and topographically lower center of the polygon and investigated the effect of snow cover accumulation on this process. During the study period, freeze-back started between September and October and ended between October and January. Between different depths, freeze-back onset was relatively stable while the duration showed more variability. Shallow depths refroze sooner than greater depths. I observed a shift between 7 d to 11 d towards later freeze-back onset at the polygon rim and center. While freeze-back duration was relatively stable in the upper part of the polygon rim, the polygon center and deeper layers at the rim showed great inter-annual variability. A notably long freeze-back duration occurred in 2015, 2016, and 2020. Meanwhile, freeze-back at the polygon center started later and took longer compared to the rim. Interestingly, the date of the first snowfall did not have a distinct impact on the freeze-back process. While the freeze-back onset was more closely connected to the air temperature, the duration was more likely influenced by snow depth, snow water equivalent (SWE), and volumetric water content (VWC). This work emphasizes the importance of gaining a more comprehensive understanding of freeze processes, their drivers, and the role of soil microtopography. It highlights the need to consider the variations in both process and drivers across different topographical features when assessing active layer conditions.

Kurzfassung

Der globale Klimawandel beeinflusst die Temperatur und die Tau- und Gefrierprozesse der Auftauschicht in arktischen Permafrostböden. Steigende Temperaturen im Permafrost wurde ausführlich untersucht, aber die Veränderungen der saisonalen Auftau- und Rückfrierprozesse wurden oft weniger beachtet. Ziel dieser Arbeit war es, die Variabilität des Einsetztens und der Dauer des Rückfrierprozesses der Auftauschicht auf der arktischen Insel Samoylov in nordost Sibirien zu untersuchen. Samoylov ist durch kontinuierlichen Permafrost und eine polygonale Tundralandschaft geprägt. Ich habe die Bodentemperatur zwischen 2014 und 2020 unter Berücksichtigung der Mikrotopographie des Polygons analysiert. Ich habe den Start und die Dauer des Rückfrierprozesses in verschiedenen Tiefen im erhöhten Rand und im topographisch tieferen Zentrum des Polygons ermittelt und den Einfluss der Schneeakkumulation auf den Prozess untersucht. Während des Untersuchungszeitraums begann der Rückfrierprozess zwischen September und Oktober und endete zwischen Oktober und Januar. In den verschiedenen Tiefen war der Start des Prozesses relativ stabil, während die Dauer größere Abweichungen aufweist. Geringe Tiefen gefroren schneller als größere Tiefen. Ich habe eine Verschiebung des Rückfrierstarts zwischen 7 und 11 Tagen in beiden Teilen des Polygons festgestellt. Die Rückfrierdauer war im oberen Teil des Polygonrandes relativ stabil, während sie im Polygonzentrum und im tieferen Teil des Randes hohe jährliche Variabilität aufwies. Die Jahre 2015, 2016 und 2020 zeigten eine auffallend lange Rückfrierdauer. Währenddessen begann der Rückfirerprozess im Polygonzentrum später und dauerte länger als im Polygonrand. Interessanterweise hatte die Schneeakkumulation keinen eindeutigen Einfluss auf den Rückfrierprozess. Während der Start des Prozesses eher mit der Lufttemperatur zusammenhing, wurde die Dauer vermutlich mehr durch die Schneehöhe, das Schnee-Wasseräquivalent und die Bodenfeuchte beeinflusst. Diese Arbeit betont die Bedeutung eines umfangreicheren Verständnisses der Rückfrierprozesse, ihrer Einflussgrößen und der Rolle der Mikrotopographie des Bodens. Sie betont die Notwendigkeit, Unterschiede der Rückfrierprozesse und ihrer Einflussgrößen unter Berücksichtigung topographischer Eigenschaften zu betrachten, um die Bedingungen der Auftauschicht angemessen bewerten zu können.

Contents

List of Figures

List of Tables

1 Introduction

Anthropogenic climate change, which encompasses more frequent and severe weather and climate extremes, has led to prevalent negative consequences for both nature and people (IPCC, 2022). The Intergovernmental Panel on Climate Change (IPCC) projects further air temperature rise and global warming to reach 1.5 °C in the near future (IPCC, 2022). This development will effectively put the Arctic region at high risk of experiencing potentially irreversible changes (Constable et al., 2022). The Arctic is already experiencing exceptional climate change impacts such as an enhanced loss of sea ice, glacier and ice sheet mass, increasing wildfires, changing snowmelt rates and periods, and permafrost thaw (Constable et al., 2022). Due to the Arctic amplification, Arctic air temperatures are on average rising more than twice as fast as the global mean (Constable et al., 2022). Arctic amplification describes the feedback process induced by global warming. As a result of rising air temperatures, snow and sea ice cover decreases. The loss of these highly reflective surfaces leads to more solar radiation being absorbed, thus amplifying further warming (AMAP, 2021). This effect is especially prevalent in autumn and winter (Constable et al., 2022). Since the polar regions serve as crucial regulators of the climate system (Constable et al., 2022) and the Arctic is a potential climate tipping element (Lenton et al., 2008), possible changes induced by further climate change will pose great risks for the global climate. Thawing permafrost is one of the multiple climatic impacts the Arctic is already experiencing, leading to critical changes for Arctic settlements and economies (Constable et al., 2022).

Permafrost is defined as earth material that remains at or below 0 °C for at least two consecutive years (Van Everdingen, 1998). It is abundant in large parts of the Northern Hemisphere (see Section 2), most of it located within the Arctic region. Global warming leads to increasing ground temperatures in permafrost regions, thus inducing permafrost thaw. This encompasses a deepening of the seasonally thawing and freezing, so-called "active layer" (Van Everdingen, 1998), with critical consequences. Permafrost degradation can impact surface stability and lead to carbon decay, inducing further climatic feedback

processes (Duchkov, 2006; Zimov et al., 2006; Schaefer et al., 2011; Schuur et al., 2015; Janowiak et al., 2017; Vincent et al., 2017).

In order to appropriately assess the challenges and mitigate the consequences caused by permafrost degradation, it is crucial to understand the interactions of permafrost with further climate and land surface characteristics. These include for instance air temperature, vegetation, precipitation, disturbance, and pollution. A better understanding of soil properties and the dynamics of the seasonal thawing and freezing processes of the active layer is important as well. Many studies have investigated permafrost and its changing characteristics in the past decades (e.g. Grigoriev, 1960; Gold and Lachenbruch, 1973; Zhang et al., 1997; Duchkov, 2006; Boike et al., 2013; Kitover et al., 2013; Vincent et al., 2017; Biskaborn et al., 2019).

A lot of attention has been drawn toward the active layer of permafrost. The seasonal thawing and freezing processes of the active layer are highly variable and closely connected to the prevalent local conditions of climate, snow cover, and soil properties such as moisture, substrate, and conductivity (Vincent et al., 2017). Furthermore, these processes behave differently at the different depths within the soil profile and are also impacted by the soil's topography. For example, phase-change processes at sites with patterned ground might show a higher spatial variability (e.g. Yi et al., 2019) than those at sites with plain surfaces. Many studies have examined the thaw- and freeze cycles of the active layer at various permafrost sites (e.g. Boike et al., 1998; Hinkel et al., 2001; Wagner et al., 2003; Park et al., 2011; Luo et al., 2014; Yi et al., 2014), but fewer studies paid detailed attention to the freeze-back process at different depths with respect to the soil's topography (e.g. Hinkel et al., 1990; Osterkamp and Romanovsky, 1997; Yi et al., 2019). While it is crucial to understand the thawing and freezing processes of the active layer as a whole, getting a detailed look at the freeze-back process itself is also important.

The Arctic amplification effect is especially strong in autumn and winter, the cold season when the soil starts to freeze. The surface warming associated with this effect could impact the timing of active layer freeze-back. Active layer freezing is also influenced by the insulating properties of snow cover (Goodrich, 1982; Zhang et al., 1997; Stieglitz et al.,

2003; Park et al., 2015; Vincent et al., 2017; Yi et al., 2019), which is expected to change due to climate warming (Stieglitz et al., 2003; Callaghan et al., 2011; Vincent et al., 2017). Thus, it is important to gain a better understanding of the active layer freeze-back process and its development in order to further estimate the current and future development of permafrost active layer conditions.

In this work, I addressed the following research questions:

- When did the active layer begin to freeze and how long did the freeze-back process take?
- In what way did the freeze-back process vary between the rim and the center of a polygon?
- How did the freeze-back behave at different depths?
- What kind of changes could be observed during the study period?

The following part of this section contains a description of the study site. Section 2 provides the theoretical background of this work and Section 3 contains the hypotheses and the data and methods I used in this work. The results of my analysis are described in Section 4 and discussed in Section 5. A summary of this work and final conclusions are given in Section 6.

1.1 Study site

The study site was located on Samoylov Island at 72°N, 126°E, which lies within the southern part of the Lena River Delta in northeastern Siberia, as shown in Figure 1. The Lena River Delta consists of 1,500 islands and three different river terraces. The first and youngest terrace was formed during the Holocene and is characterized by a polygonal tundra landscape with thermokarst lakes and an active floodplain. The second terrace developed between the early Holocene and late Pleistocene and consists of sandy sediments and thermokarst lakes. The third terrace is the oldest river terrace of the Lena

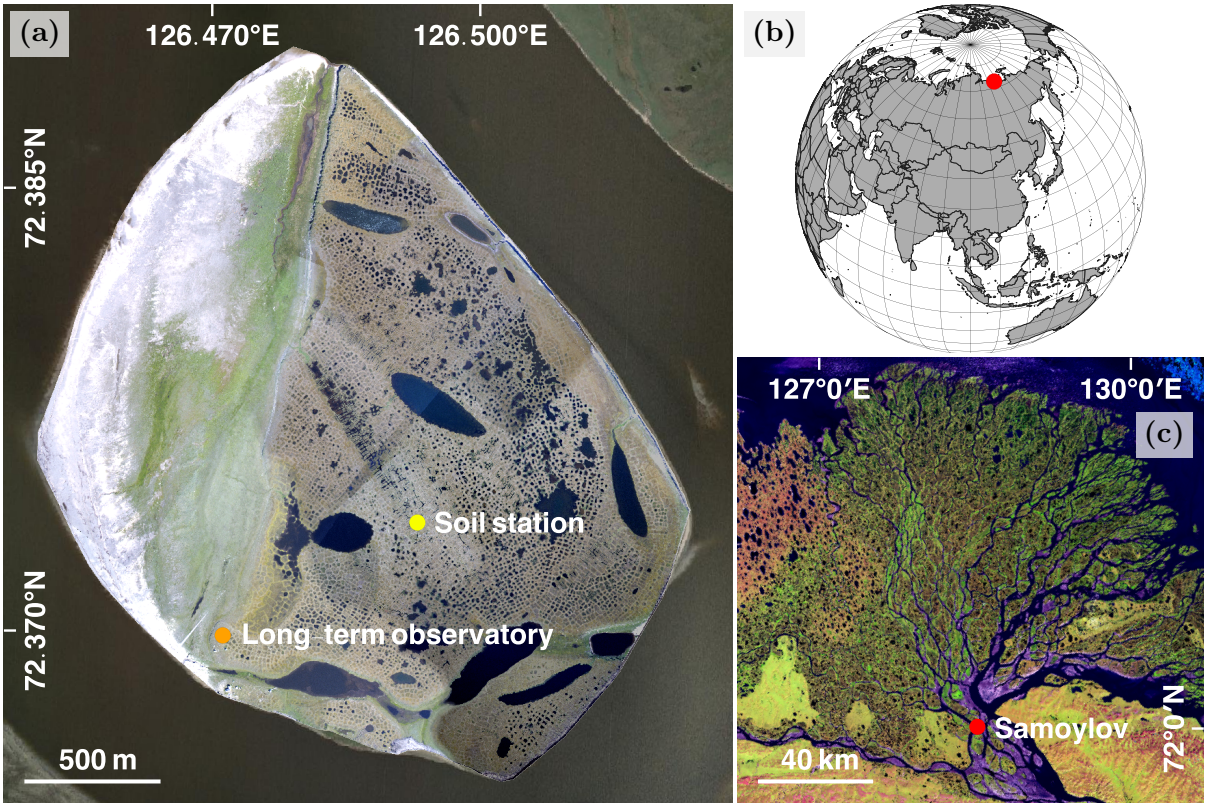

Figure 1: Overview of the study site. (a) The soil measurement station (yellow circle) is located in the central part of Samoylov Island. The long-term observatory (LTO, orange circle) lies in the southwestern part of the island. Soil temperature data were obtained from the soil station, reference air temperaure data from the LTO (Boike et al., 2022). The orthomosaic of the island was produced by Boike et al. (2012). (c) Samoylov lies within the southern part of the Lena River Delta, which is shown as a false-color satellite image from July 27, 2000 (NASA Landsat Program, 2000). (b) The Lena River Delta is located in northeastern Siberia.

River Delta. It was formed in the late Pleistocene and is characterized by patterned ground and fine, organic, and ice-rich sediments (Grigoriev, 1993; Schwamborn et al., 2002).

Samoylov Island is located on the first river terrace and covers an area of about 4.5 km^2 (Morgenstern et al., 2008). The region's defining feature is its Arctic continental climate, which includes low mean annual air temperatures below −12 °C, extremely cold minimum winter air temperatures below −45 °C, and summer air temperatures that can rise above 25 °C (Boike et al., 2013). The landscape on Samoylov Island is characterized by patterned

ground. It consists mainly of polygonal tundra, including ice-wedge polygons with wet, topographically lower centers and drier, elevated rims, as well as water bodies such as thermokarst lakes and ponds (Muster et al., 2012; Boike et al., 2013). The vegetation on the island is composed of wet and dry tundra and water surfaces, including plants such as mosses, shrubs, lichen, and grasses (Muster et al., 2012; Boike et al., 2013). The area is underlain by continuous permafrost reaching down to 400 m to 600 m below the surface (Grigoriev, 1960) with an active layer that starts to thaw at the end of May and reaches its maximum thickness between late August and early September (Boike et al., 2019).

Continuous measurements of soil parameters and meteorological conditions have been conducted at this site since 1998 (Boike et al., 2013). The measurement station that provided the soil temperature data used for this work was set up in a low-centered polygon in August 2012. This is a different station than the long-term observatory (LTO) described by (Boike et al., 2019), see Figure 1a. Data were available until September 2021. Sensors for measuring soil parameters were installed both at the rim and center of the polygon. Further explanation of polygons as permafrost features can be found in Section 2.

2 Theoretical background

In this section, I provide the theoretical background for my work. First, I describe the thermal state of permafrost, the active layer, and its importance for the global climate. After that, I give further information on polygons, the characteristic permafrost features at the study site, and explain the role of snow cover in permafrost regions.

2.1 Thermal regime of permafrost

Permafrost, defined as earth material at or below 0 °C for at least two consecutive years (Van Everdingen, 1998), can consist of rock, sediment, or soil. It covers about 13 % to 18 % of the exposed land surface in the Northern Hemisphere (Obu, 2021), whereas the majority is found in the polar regions. Based on the degree of its spatial continuity, permafrost can be separated into continuous (more than 90 %), discontinuous (50 % to 90 %), and

sporadic (10 % to 50 %) permafrost (Vincent et al., 2017). It can be found on land and below the seabed and its depth varies between a few centimeters to several hundreds of meters. Characteristics of permafrost such as depth, distribution, and temperature depend on local factors, for example air temperature, vegetation, snow cover, and glacial history (Boike et al., 2013).

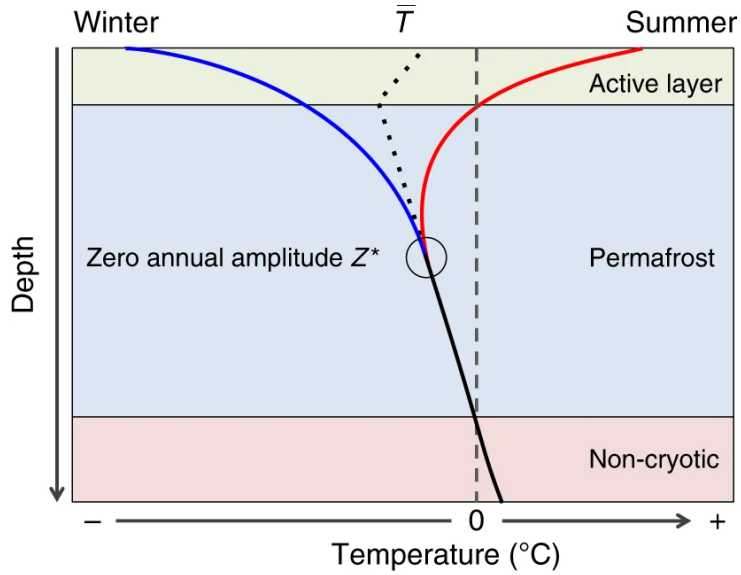

Figure 2: Schematic showing the thermal regime of permafrost. The red line indicates the maximum, and the blue line the minimum ground temperature during the year (Biskaborn et al., 2019).

The thermal regime of permafrost can be described with a temperature curve, as shown in Figure 2 (Biskaborn et al., 2019). Maximum and minimum soil temperatures, usually absolute temperatures over the period of one year, are plotted against the depth of the soil. The temperature amplitude decreases with increasing depth until the temperature curves meet at the depth of zero annual amplitude (Biskaborn et al., 2019), where the mean annual soil temperature varies by less than 0.1 °C. Towards greater depths, the soil temperature rises above 0 °C due to the geothermal gradient (Van Everdingen, 1998). The active layer is the upper soil layer which seasonally thaws in summer and freezes back in fall. It can be a few centimeters to several meters thick and is directly influenced by local variations in air temperature, snow, vegetation, volumetric water content (VWC), and ice content (Boike et al., 2019).

Increasing permafrost temperatures have been observed across continuous permafrost regions (Biskaborn et al., 2019). Permafrost thaw encompasses a deepening of the active layer. Its depth varies across different permafrost regions and is projected to increase further in the future (Constable et al., 2022). During the setup of the soil station in August 2012, the active layer depth ranged between approximately 30 cm at the polygon rim and 45 cm at the polygon center (retrieved from Figure 3). The pronounced and projected permafrost thaw is critical for various reasons. For example, it can impact surface stability and thus be harmful to infrastructure built on surfaces that are underlain by permafrost, such as buildings, railways, roads, and pipelines (Duchkov, 2006; Constable et al., 2022). Furthermore, permafrost contains about 1,600 gigatons of carbon, which is approximately twice the amount of carbon that is stored in the atmosphere (Janowiak et al., 2017). This carbon, usually the remains of plants and animals (Schuur et al., 2015), is preserved in the frozen soil and consequently protected from decay (Janowiak et al., 2017). Thawing permafrost exposes this organic carbon, therefore enabling it to be decomposed by soil microbes (Schuur et al., 2015) which further induces the permafrost-carbon feedback (Zimov et al., 2006; Schaefer et al., 2011; Schuur et al., 2015; Janowiak et al., 2017). Carbon decay leads to the formation and release of additional carbon dioxide and methane into the atmosphere. These greenhouse gases further contribute to air temperature and surface warming, in turn enhancing permafrost thaw.

The active layer freeze-back process was the objective of this work. Freeze-back is connected to the soil's water content (Gold and Lachenbruch, 1973; Outcalt et al., 1990; Romanovsky and Osterkamp, 2000; Luo et al., 2014; Zhao et al., 2022). When air temperature begins to rise in summer, soil temperature increases and the frozen active layer begins to thaw. Therefore, the volumetric water content of the soil increases. In fall, when air temperature decreases, the soil temperature gradient is less steep. This is due to the liquid water contained in the unfrozen soil. During the phase change of liquid water to ice latent heat is released, which leads to a soil temperature of approximately 0 °C for several days or even weeks. After the majority of the water is frozen, soil temperature drops below 0 °C again. This effect is also referred to as the zero-curtain effect (Outcalt

et al., 1990) and the duration of freeze-back can therefore be referred to as the zero-curtain period.

Previous research conducted on Samoylov Island focused on the thawing period of the active layer, which was observed to start towards the end of May and last until late August to early September (Boike et al., 2019). Freeze-back has been found to generally start towards the end of September (Langer et al., 2011b). However, global climate change affects the soil temperature and soil moisture, which is why I expected to observe changes in the freeze-back process of the active layer.

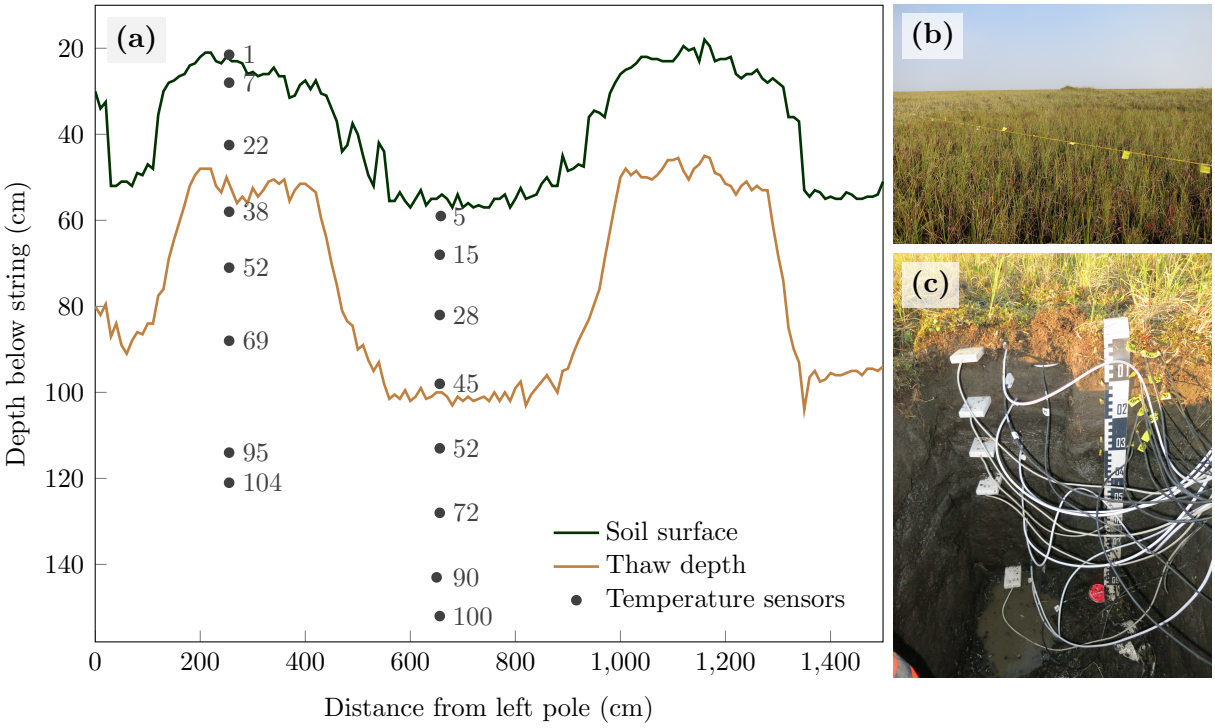

Figure 3: (a) Profile of the polygon at the study site. The polygon was measured in August 2012 at instrument setup. The green line indicates the soil surface, which was measured relative to a string that was taut across the polygon (b, taken by Julia Boike). The brown line indicates the thaw depth, hence the active layer thickness at the time of setup. The gray dots indicate the soil temperature sensors that were installed at the rim and center of the polygon as well as their depths relative to the surface (c, taken by Julia Boike). The white bars in (c) are time-domain reflectometer (TDR) sensors for measuring the soil's volumetric water content (VWC). Soil temperature sensors were installed to the right of the TDR sensors. Data were provided by Julia Boike's working group at Alfred Wegener Institute.

2.2 Polygonal patterned ground

The investigated part of Samoylov Island is characterized by polygonal patterned ground which has developed over the course of several hundred years (de Koven Leffingwell, 1915; MacKay, 2000; Boike et al., 2013). Extreme cold temperatures in winter cause the soil to contract and form vertical frost cracks in pentagonal, orthogonal, or hexagonal networks (de Koven Leffingwell, 1915; Lachenbruch, 1962, 1963). These frost cracks get infiltrated by water from melting snow or rain, which freezes and leads to ice-wedge formation in the cracks (de Koven Leffingwell, 1915). During summer, the frozen soil thaws and expands. Because of the ice-wedges the soil cannot expand horizontally and either bulges up as a whole or only next to the ice-wedges. In the latter case, the soil forms elevated rims and topographically lower centers. This process repeatedly occurs over the course of several hundred years until low-centered polygons develop (de Koven Leffingwell, 1915; MacKay, 2000; Boike et al., 2013). A schematic cross-section of low-centered ice-wedge polygons and pictures of the polygonal network on Samoylov Island are shown in Figure 4. The centers of these polygons are often wet or water saturated. A profile of the specific polygon where the measurement instruments were set up is shown in Figure 3. As shown in this figure, the distance between the polygon rim and center is approximately 4 m. With respect to the center, the rim is elevated by approximately 30 cm.

2.3 The role of snow cover in permafrost regions

The temperature of permafrost soils is not just dependent on the surrounding air temperature. In fact, the soil temperature in zones of continuous permafrost differs significantly from the air temperature due to the influence of snow cover and other near-surface factors such as vegetation or topography (Gold and Lachenbruch, 1973). According to model findings, changes in near-surface air temperature can have an equal impact on changes in below-ground temperature as temporal differences in snow cover (Stieglitz et al., 2003). Previous research has shown that snow cover has a substantial impact on the soil temperature of continuous permafrost in northernmost regions such as northeastern Siberia

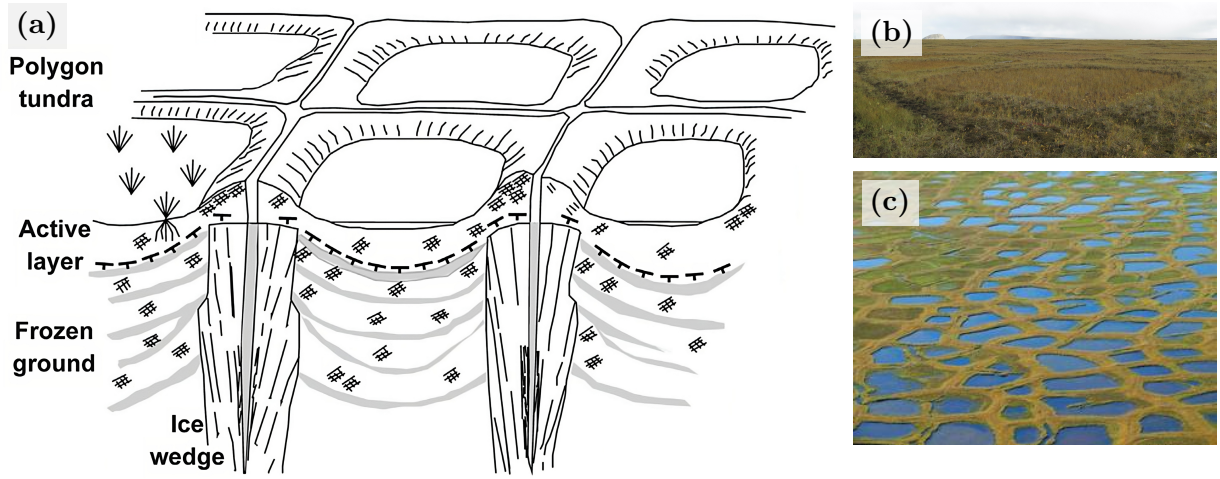

Figure 4: (a) Schematic cross-section of polygonal tundra in the Lena River Delta, Siberia. The polygons are low-centered with elevated rims. From Wetterich et al. (2014) after Romanovskii (1977). (b) View of a low-centered polygon from the ground (taken by Julia Boike). (c) Aerial photo of water-saturated low-centered polygons on Samoylov Island (taken by Konstanze Piel).

(Park et al., 2015). As part of ongoing climate change, changes in the timing, depth, and duration of snow cover are expected, although with large regional variability (Stieglitz et al., 2003; Callaghan et al., 2011; Constable et al., 2022). These changes may exert a potential influence on permafrost temperatures.

Snow can insulate the soil and therefore affect its temperature, which is especially significant in regions at higher latitudes (Park et al., 2015). Particularly fresh snow has a very high albedo and reflects about 80 % of the incoming solar radiation (Vincent et al., 2017). Combined with its low thermal conductivity, fresh snow insulates the soil and creates a thermal offset between the soil temperature and the air temperature (Park et al., 2015; Vincent et al., 2017), which leads to an increase of the average annual soil temperature (Goodrich, 1982; Zhang et al., 1997). Thus, snow conditions in early winter are critical to the soil temperature (Goodrich, 1982). This was important for my analysis because snow cover accumulation and onset of active layer freeze-back occured at about the same time at the study site. It was thus interesting to investigate the potential effect of snow cover on the freeze-back process and how this effect varied between the polygon rim and center. For instance, Yi et al. (2019) found that an early snow accumulation re-

sulted in a delayed onset of active layer freeze-back and an extended freeze-back duration. However, the rate and duration of snow accumulation as well as the amount and density of the snow potentially influence its insulating effect on the soil (Stieglitz et al., 2003; Yi et al., 2019). Due to the influence of wind and topography (Zhang et al., 1997; Boike et al., 2013), snow cover might significantly differ between the polygon rim and center, even during snow cover build-up. As part of this analysis, I focused on the impact of the start of snow cover accumulation on the active layer freeze-back onset and duration.

3 Methods

In this section, I describe the hypotheses that I formulated prior to the analysis. I provide details on the used data and their quality control as well as the methods that I applied to estimate the active-layer freeze-back onset and duration.

3.1 Hypotheses

Bearing in mind the theoretical background and the climatic development stated above, I formulated three hypotheses for the analysis. Over the course of the study period, from 2014 to 2020:

- The onset of freeze-back experienced a delay at both the polygon rim and center.
- The duration of freeze-back increased at both the polygon rim and center.
- Freeze-back started later at the polygon center and took more time compared to the polygon rim.

3.2 Data and quality assurance

3.2.1 Soil temperature

Data on soil temperature were available from 2012 to 2021 and were obtained from the soil station shown in Figure 1a). Data were provided by Julia Boike's working group at

Alfred Wegener Institute. The sensors for the measurement of the soil temperature were installed at different depths at the rim and center of the polygon (Figure 3). Sensors were installed at 1 cm, 7 cm, 22 cm, 38 cm, 52 cm, 69 cm, 95 cm, and 104 cm at the polygon rim and at 5 cm, 15 cm, 28 cm, 45 cm, 52 cm, 72 cm, 90 cm, and 100 cm at the polygon center. The depths were measured relative to the polygon's surface. Soil temperature data were measured with a temporal resolution of 30 minutes.

In order to provide good-quality data for the analysis, I performed a quality check for the soil temperature data following the flagging system implemented by Boike et al. (2019) and only used data with good quality (flag 0). Further explanation of the quality flagging system can be found in the appendix in Table A1. The time frame of the data set ranged from August 2012 to September 2021. Due to instrument setup induced unreliability in 2012 and missing data in 2013, I shortened the data set to begin in April 2013. Subsequently, I resampled the data from a temporal resolution of 30 minutes to mean hourly values. I filled short data gaps of up to six hours with linear interpolation. Figure 5 shows an example of the gap interpolation for the soil temperature sensor at 5 cm at the center of the polygon. A summary of the results of the gap treatment for all soil temperature sensors is given in the appendix in Figure A1. The data set included a few large data gaps which could not be filled since they were longer than six hours (Figure 6).

3.2.2 Air temperature

Data from the soil station included measurements of meteorological parameters such as air temperature. As there were some large gaps in this data set, I used reference air temperature data from the long-term observatory (Figure 1a). These data can be obtained from PANGAEA (Boike et al., 2022) with a temporal resolution of one hour and are available since 1998.

The reference air temperature data were level 2 data that had already been quality checked (after Boike et al., 2019) and compiled to hourly resolution. Only data with good quality (flag 0) were published on PANGAEA. I aggregated the data to mean daily values

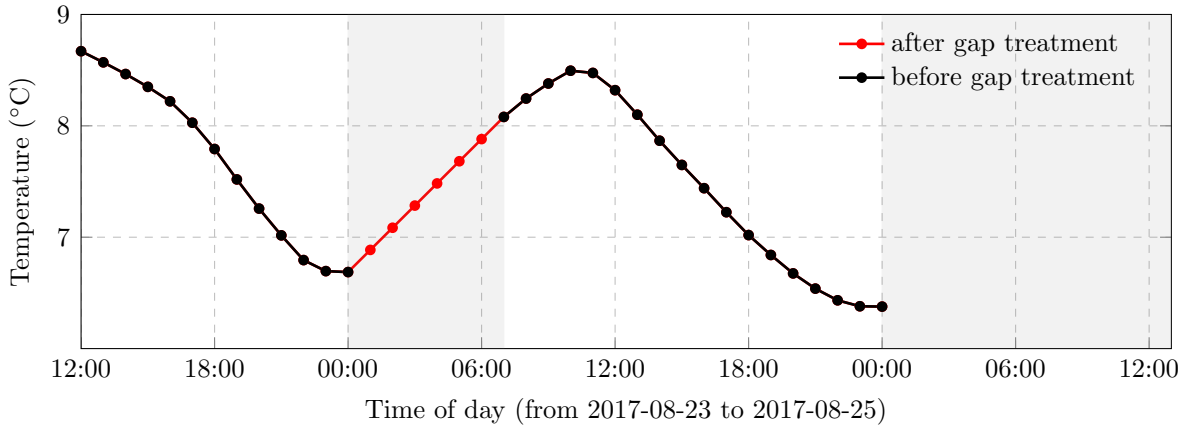

Figure 5: Example of the gap treatment for the soil temperature data. The figure shows the soil temperature measured at the center of the polygon at 5 cm depth from August 23 2017 12:00 to August 25 2017 12:00. Time is given in coordinated universal time (UTC). Local solar altitude is approximately 8.5 hours before UTC. The black dots indicate the measured soil temperature before, and the red dots indicate the soil temperature after the gap treatment. The first gap of missing values could be filled with linear interpolation. The second gap shown in this figure could not be filled as it was longer than six hours.

and treated data gaps by applying linear interpolation for gaps of up to six hours if at least 12 hourly values were available for the day. Otherwise, I did not calculate the mean daily air temperature. Subsequently, I applied linear interpolation for the daily data set for gaps of up to six days.

3.2.3 Snow accumulation

I estimated the start date of snow accumulation for each year from webcam images of the site. The images were provided by Julia Boike's working group at Alfred Wegener Institute. My purpose was to estimate the onset of snow accumulation each year, which I defined as the date on and after which the study site stays continuously snow-covered. This did not indicate a snow coverage of 100 %. It was rather defined as the date after which there were no snow-free periods anymore until spring. First, I visually approximated the spatial snow coverage in percent for every available date with an accuracy of 5 %. Subsequently, I estimated the start of snow accumulation based on maintaining or increasing snow coverage. Based on that, I calculated the day of the year when snow

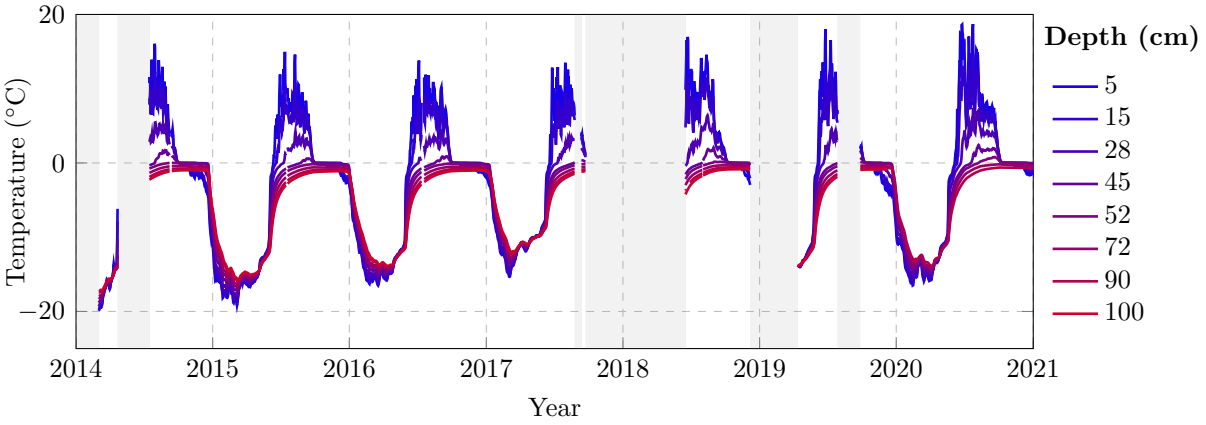

Figure 6: Soil temperature time series measured at the center of the polygon. The lines indicate the mean daily soil temperatures at different depths. The gray rectangles mark data gaps that could not be filled because they were too long to be interpolated. Some of these gaps influenced the analysis and limited the results, as data in critical time periods for the analysis were missing.

accumulation started. Figure 7 shows examples of these webcam images with different snow cover conditions.

Due to my visual and manual approach to estimating the start of snow accumulation, these data could not be assigned to a specific quality level. Webcam images were not available for every single day and were often blurry or not usable, especially during the polar night. The snow accumulation data set was valuable as it represented the only available source of spatial information despite some restrictions, such as winter darkness, blurry, and missing images. I had the possibility to use measurement data on snow depth from an acoustic snow depth sensor at the soil station. However, these data were not optimal for the purpose of this work. Due to for instance vegetation growth, the soil surface was not well defined and a shallow and patchy snow layer could not reliably be determined. Furthermore, I was interested in the spatial characteristics of the snow, not the discrete point scale. Since I looked at several polygonal landscape units, webcam images were the preferable data source for this purpose.

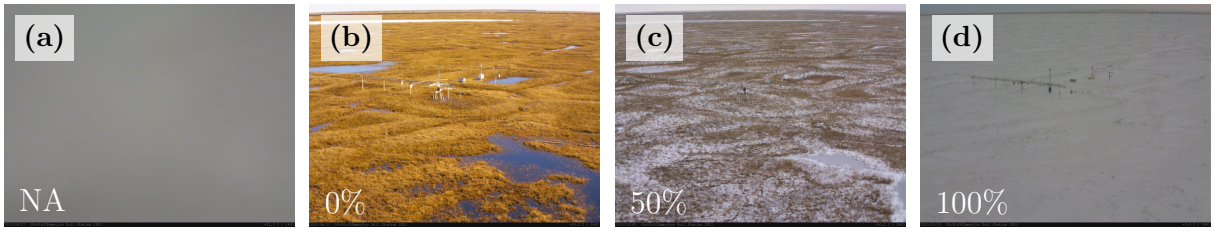

Figure 7: Examples of snow cover classification based on webcam images. These images were obtained from a 10 m high tower and frame the study site. (a) Example of a low-quality image on 2020-05-27. In this case, I defined the snow cover data as not available (NA). Other NA cases involve images taken during the (polar) night, corrupt images, and missing images. (b) Image taken on 2020-05-12. All the snow has melted, therefore I classified the snow cover as 0 %. (c) The site is partly snow-covered on 2020-10-05 with a thin snow cover across the whole site but a lot of grasses and shrubs are still visible. Therefore, I defined the spatial snow cover as 50 %. (d) The entire site is overlain by a layer of snow on 2020-10-31, I defined the snow cover as 100 %. The webcam images were provided by Julia Boike's working group at Alfred Wegener Institute.

3.3 Analysis

I conducted the analysis with Python 3.9.14. and prepared the data as described above. The script was provided by Inge Grünberg at Alfred Wegener Institute and was originally written for a research site in Svalbard, Norway. I made adaptations to the script to fit the data set obtained from the soil station at Samoylov and analyzed the soil temperature data as follows:

I created a time series for which I identified the condition of the soil based on its temperature to be either warm, cold, very cold, NaN (no data), or in the phase-change (zero-curtain) condition and then filled the gaps for the temperature conditions. The thresholds for identifying and filling the temperature conditions are listed in Table 1. Subsequently, I removed periods too short to be relevant by smoothing the conditions with simple forward fill and computed annual statistics for the soil temperature conditions. I only saved the results if the respective periods were well represented by the data series.

Table 1: Thresholds for identifying soil temperature (T_s) conditions and for filling the data gaps in the temperature conditions. I adapted these thresholds from the original script. I determined the zero-curtain threshold ($-0.2\,°C$) based on T_s and VWC curves at the study site. Under the given respective T_s or air temperature (T_{air}) condition, gaps were filled with simple forward fill. This means that missing values were filled based on the previous value.

Soil temperature condition	**Threshold for identifying condition**
warm	$T_s > 0.1\,°C$
cold	$-0.2\,°C > T_s >= -2.5\,°C$
very cold	$T_s < -2.5\,°C$
zero-curtain	$0.1\,°C >= T_s >= -0.2\,°C$
Soil temperature condition gap	**Threshold for filling gap**
short breaks (<= 10 days)	before == after
medium breaks (<= 20 days)	before == after AND winter (December-June)
winter breaks (starting very cold)	Reference $T_{air} <= -1.2\,°C$
winter breaks (starting cold)	Reference $T_{air} <= -1.2\,°C$
end of winter breaks ending with hard frozen	last Reference $T_{air} < -8\,°C$
gaps < 24h	simple forward fill

3.3.1 Onset and duration of freeze-back

I calculated the onset of freeze-back each year based on the soil temperature to drop to $0.1\,°C$ and maintain within the zero-curtain threshold (Table 1). I defined the end of freeze-back as the day of the year (DOY) which was followed by at least 10 d of consecutively cold conditions. In particular close to the surface soil temperature often drops below $0\,°C$ and spontaneously rises above $0\,°C$ again. The threshold of at least 10 d of consecutively cold conditions ensured that the soil was frozen. If the calculated date fell within the subsequent year, it was still attributed to the current year. I calculated the duration of freeze-back in days by subtracting the start of freeze-back DOY from the end of freeze-back DOY.

Due to missing soil temperature data in the freezing season in 2013 and 2021, results

on the active layer freeze-back were only available from 2014 to 2020. For this period, I compared the onset and the end or duration of freeze-back between the rim and the center of the polygon for the respective years of the observation period. I calculated the absolute (and percentage) change between the respective years for each depth. In order to compare the different depths of the rim and center of the polygon, I had a detailed look at the year 2016. This was the only year for which data for all measured depths at the rim and center of the polygon were available. Additionally, I investigated the possible influence of the start of snow accumulation on the freeze-back onset and duration.

4 Results

This section contains the results of my analysis. First, I examine the seasonal temperature variations with depth at both the rim and center of the polygon, as well as the relationship between air temperature and soil temperature over the course of one year (2016). Then, I describe the results for the freeze-back onset and duration over the course of the study period (2014-2020). I pay special attention to the inter-annual variability and the development during the study period, as well as the variability between the different depths. Due to a large data gap between 2016 and 2018, only few results for 2017 were available. The time series was too short to calculate or provide reliable trends so that I only describe the results with respect to the length of the time series.

4.1 Soil temperature profile in 2016

Figure 8 shows the mean daily soil temperatures at the rim and center of the polygon and the reference air temperature for the year 2016. As described in Section 2, there was a distinct offset between the air temperature and the soil temperature. This offset could be observed at the rim and center of the polygon.

Rim: At the beginning of the year, the air temperature was between $-20\,^{\circ}\mathrm{C}$ to $-30\,^{\circ}\mathrm{C}$, and the soil in the polygon rim was completely frozen with temperatures of approximately

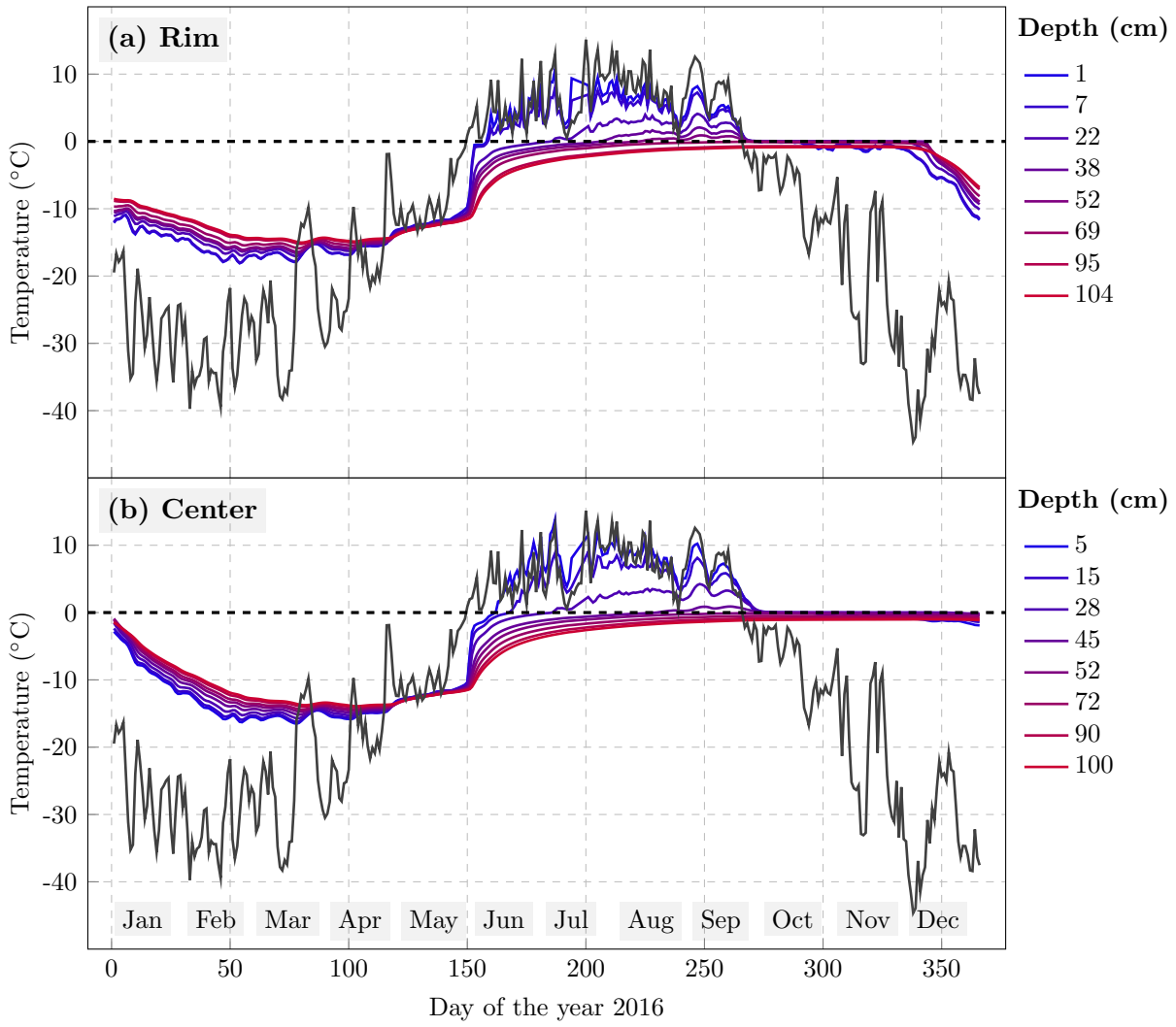

Figure 8: Temperature profile at the measured depths in 2016 at the polygon rim (a) and center (b). Temperatures were gap-filled and aggregated to daily values. The gray line indicates the air temperature at 200 cm height that was measured at the Samoylov long-term observatory.

−8 °C to −12 °C (Figure 8a). There was still some variability between the daily temperature values, especially for the depths closer to the surface. These shallow depths had a lower temperature than greater depths. At all depths, the soil temperature continued to decrease until approximately the beginning of March. At that time, the air temperature began to rise with large fluctuations. Shortly after the air temperature began to rise, the soil temperature at all depths slowly increased, followed by a rapid increase starting at the end of May. The soil temperature at shallow depths exhibited the most rapid increase

and reached the highest temperatures, followed by the intermediate depths. While the soil above 95 cm thawed in spring, the deeper layers warmed but remained at or below 0 °C and maintained this level for the majority of the rest of the year. While in the thawed state, the soil temperature close to the subsurface reached values close to the air temperature. Towards late September the air temperature dropped to negative values and continued to decrease. The soil temperature at thawed depths dropped almost simultaneously but did not decrease as fast as the air temperature. Instead, it remained at a level of approximately 0 °C for a substantial amount of time, the zero-curtain period. In late November the soil temperature at all depths decreased, whereas a stronger temperature decrease occurred at shallow depths. At the end of the year, the soil was frozen at all depths, although the soil temperature had not decreased to the same level as observed at the start of the year.

A closer look at the start and end of the freeze-back in 2016 (Figure 9a) showed that the timing of freeze-back onset was relatively stable for the different depths and only varied by about 2 d, whereas the end of freeze-back was more variable and differed by up to 53 d. The earliest end of freeze-back occurred at the shallowest depths. Interestingly, the timing of freeze-back end did not increase with depth. The latest timing occurred at an intermediate depth at 38 cm. End of freeze-back at 54 cm and especially at 69 cm depth was reached much sooner than at 38 cm. Thus, the onset of freeze-back was relatively stable while the duration of freeze-back was highly variable between different depths. The shortest freeze-back duration occurred at 1 cm and at 7 cm and took 22 d, whereas the longest duration occurred at 38 cm and took 75 d. The value for the start of freezing at 69 cm was missing, hence I could not make assumptions about the length of the zero-curtain period. The depths below 69 cm are not shown in this plot. Despite seasonally rising soil temperatures, the soil at these depths remained perennially frozen.

Center: At the beginning of 2016, the soil temperature at the center of the polygon averaged to approximately −1 °C to −3 °C and was therefore about 10 °C warmer compared to the polygon rim (Figure 8b). Similar to the rim, shallow depths had colder tempera-

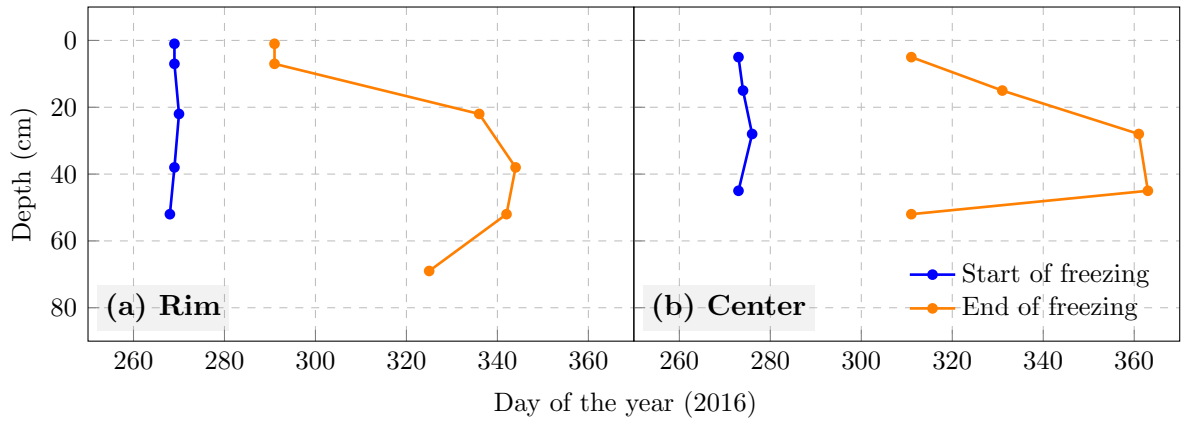

Figure 9: Start and end of freezing at the respective depths in 2016 at the polygon rim (a) and center (b). I calculated the variables as described in Section 3.

tures than greater depths. The soil temperature at all depths continued to decrease until early March, when it reached similar levels compared to the polygon rim. The dynamic of rising air temperature followed by first slowly and then rapidly increasing soil temperatures at all depths was similar as well. Soil layers above 72 cm began to thaw in spring, while deeper layers remained frozen and at a similar temperature level. It seems that at both, the polygon rim and center, soil temperature during the thawed state was closely connected to the air temperature. Thus analogous to the polygon rim, the temperature at thawed depths dropped as soon as air temperature decreased again, but remained in the zero-curtain state. However, the zero-curtain period was longer at the polygon center. Only at the end of the year the soil temperature decreased at all depths. This indicates that the end of freeze-back in 2016 at the polygon center was reached later than at the polygon rim.

Figure 9b shows that the freeze-back onset at the polygon center generally started a few days later than at the rim, with a maximum difference of 8 d. Similar to the rim, the variability between the different depths was very low, as the timing of freeze-back onset only varied by a maximum of 3 d. Additionally, a similar pattern in the timing of the freeze-back end occurred. It varied by up to 52 d, whereas the earliest end of freeze-back was reached at the shallowest depth at 5 cm, followed by the intermediate depths. However, the greatest depth in this statistic (52 cm) reached the end of freeze-back at

the same time as the shallowest depth. The value for the start of freeze-back at 52 cm was missing, thus I could make assumptions about the freeze-back duration at this depth. Values for depths below 52 cm are not included here because they remained perennially frozen.

In general, the end of freeze-back at the center was reached later than at the rim, with a difference of 20 d between the earliest and 19 d between the latest timing of freeze-back end. The duration of freeze-back took between 38 d at 5 cm and 90 d at 45 cm, thus longer than at the polygon rim. In conclusion, the variability between different depths at the polygon center was similar to the rim, for both the start and end of freeze-back, but the timing itself was shifted. The freeze-back at the polygon center started later and took longer, with a difference of 16 d between the shortest, and 15 d between the longest freeze-back duration in 2016.

4.2 Onset of freeze-back

Figure 10 shows the results for the onset of freeze-back at the rim and center of the polygon at the respective depths. Detailed results and the calculated absolute change between the consecutive years are listed in the appendix in Table B1. Freeze-back at the polygon rim and center generally started between the middle of September and the middle of October.

Rim: Figure 10a shows the onset of freeze-back at the polygon rim from 2014 to 2020 for the respective depths. In 2014 and 2015 the freeze-back started at approximately the same time with a maximum variability of 3 d between the different depths (between day 265 and 268). At 7 cm depth the freeze-back started 1 d earlier than in 2014 and started 1 d later at 1 cm. At the other depths, the freeze-back onset did not change between these two years. In 2016, the freeze-back onset was delayed at all depths between 1 d to 3 d. In 2017, the process started between 4 d to 6 d earlier than in the previous year. This year's freeze-back onset was the earliest observed throughout the study period. In 2018, the onset was delayed by 8 d to 9 d compared to 2017, and by 2 d to 4 d compared to 2016.

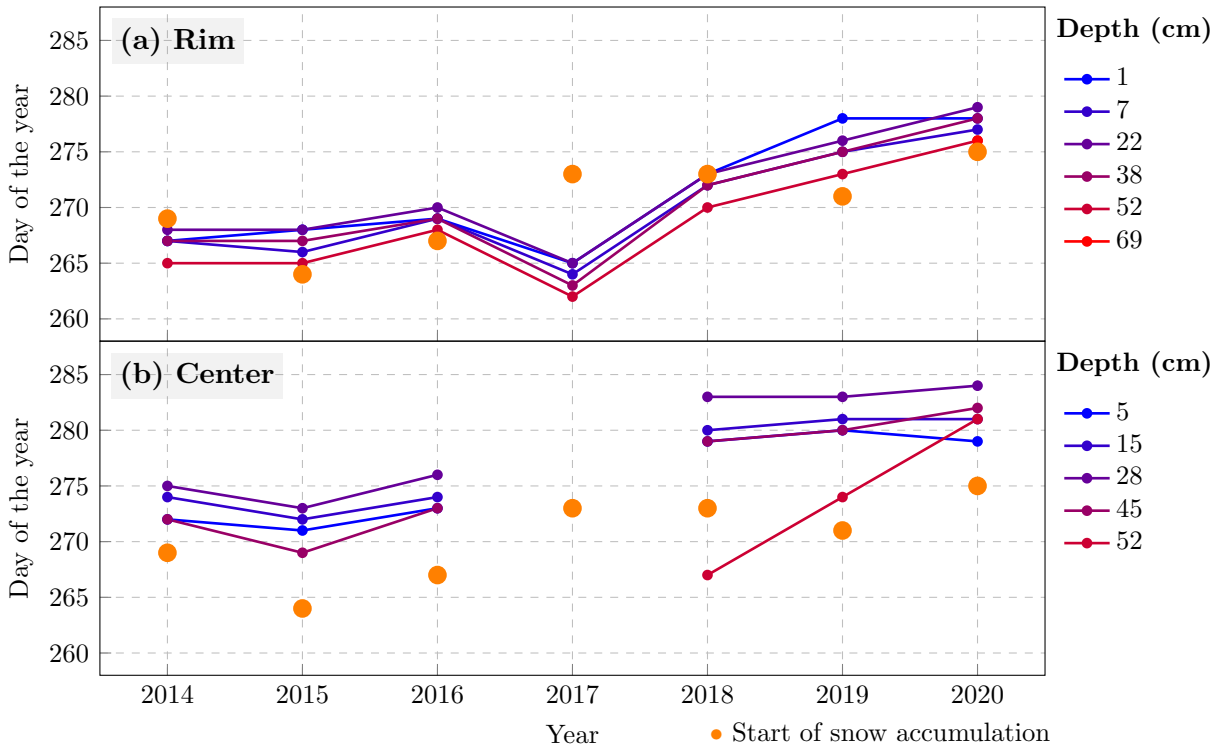

Figure 10: Onset of freeze-back at the respective depths at the polygon rim (a) and center (b) during the study period. The orange dots represent the day of the year when snow accumulation starts.

In the consecutive years, the onset was delayed by a smaller degree. Freeze-back in 2019 started between 3 d to 5 d later than in 2018, and up to 3 d later in 2020. This indicates that the early onset of freeze-back observed in 2017 was unusual.

Except for that year, the timing of freeze-back onset increased at all depths during the study period, with an absolute delay of 10 d to 11 d from 2014 to 2020 at the respective depths. Within the soil profile, freeze-back onset was relatively stable, as it only varied by a few days between the different depths in the respective years.

Center: Figure 10b shows the onset of freeze-back at the polygon center for the respective depths. Freeze-back at the polygon center generally started later than at the polygon rim. In 2014, freeze-back onset occurred approximately one week later than at the rim (between day 272 and 275). In 2015, soil freezing started between 1 d to 3 d earlier than in 2014

opposing to the rim, where the onset started at about the same time compared to the previous year. In the following year, 2016, the freeze-back onset was again delayed at all depths by 2 d to 4 d and started between day 273 and 276. Due to missing data, no results were available for 2017 at the polygon center. In 2018, freeze-back onset was delayed at all depths by 6 d to 7 d compared to 2016. From 2014 to 2016 results were only available for the depths down to 45 cm. Starting in 2018, results for 52 cm were available as well. This indicates that the soil temperature at 52 cm exceeded the zero-curtain threshold defined in Section 3 and was thus no longer permafrost, but part of the active layer. Apart from that, freeze-back at this depth started much earlier, on day 267, than at the other depths. From 2018 on, the freeze-back onset between 5 cm and 45 cm was relatively stable opposing to the polygon rim, where it kept being delayed. In 2019, freeze-back at the polygon center either started on the same day or 1 d later than in 2018. Similar to that, freeze-back in 2020 started between 1 d earlier to 2 d later than in the previous year. However, at 52 cm, freeze-back onset was delayed by 7 d in 2019 and 2020, respectively.

Summing up, freeze-back onset at the polygon center showed a slightly different pattern compared to the polygon rim. While I observed a similar variability between the different depths, freeze-back at the polygon center generally started a few days later than at the polygon rim. Furthermore, from 2014 to 2020, I detected an absolute delay of 7 d to 10 d between 5 cm and 45 cm. Thus, the delay of freeze-back onset at the polygon center was actually slightly smaller than at the polygon rim.

Influence of snow cover: The orange dots in Figure 10 represent the start of snow accumulation for the respective years. Snow accumulation generally started between late September and early October which is also shown in Figure 11. The offset between the start of snow accumulation and the freeze-back onset at the polygon center was larger compared to the polygon rim. I observed an unexpected late start of snow accumulation in 2017, which coincided with the early start of freeze-back observed at the polygon rim in that year.

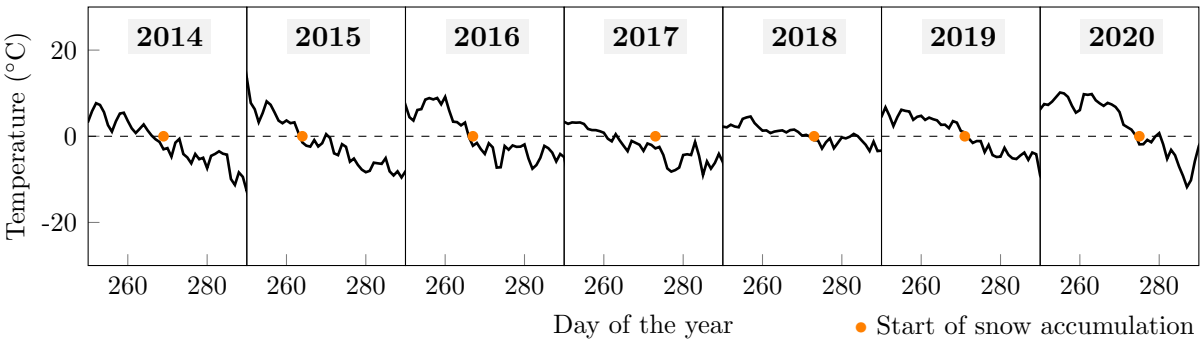

Figure 11: Mean daily air temperature during the onset of the freeze-back period. The black line indicates the air temperature at 200 cm height that was measured at the LTO. The orange dots represent the start of snow accumulation in the respective year.

A scatter plot of the freeze-back onset and start of snow accumulation is shown in Figure 12. I observed a positive relation between the freeze-back onset and the start of snow accumulation for almost every year at the polygon rim and center. Only 2017, which is marked in Figure 12a, showed a negative relation, hence a late start of snow accumulation in line with an early freeze-back onset at the polygon rim. The marked data point in Figure 12b shows the freeze-back onset of the freshly degraded permafrost at 52 cm in 2018 at the polygon center.

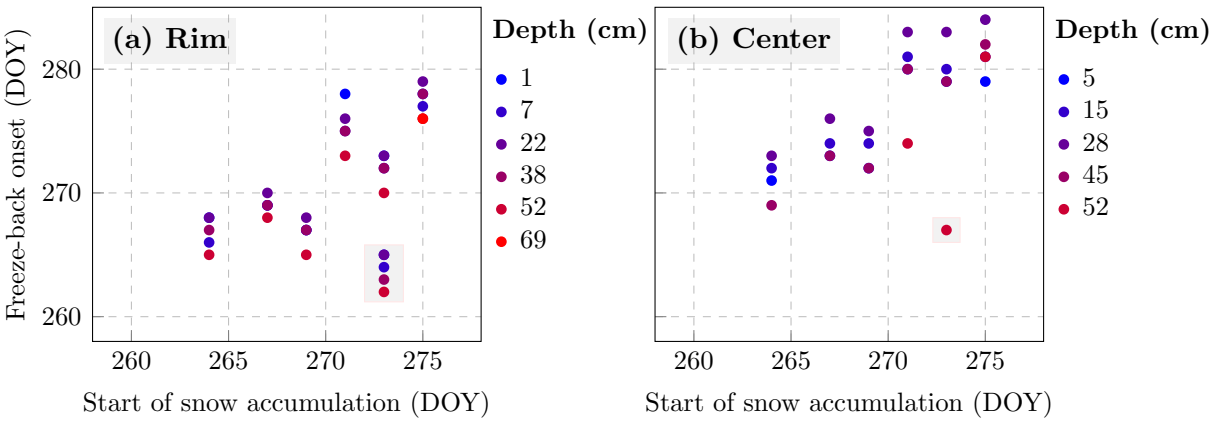

Figure 12: Freeze-back onset depending on the start of snow accumulation at the respective depths at the polygon rim (a) and center (b). The variables are depicted with the unit "day of the year" (DOY) for the entire time series. Results for the freeze-back onset at the rim in 2017 are marked in (a). The marked data point in (b) represents the freeze-back onset of the freshly degraded permafrost at 52 cm in 2018.

The freeze-back onset showed a stronger positive relation with the decreasing air temperature (Figure 13), indicated as the day when the air temperature dropped below 0 °C. The sooner this drop occurred, the sooner the freeze-back started. This relation was especially distinct at the polygon rim, for every year, including 2017. At the polygon center, the relation between freeze-back onset and air temperature (Figure 13b) was also slightly more distinct than the relation between freeze-back onset and snow accumulation (Figure 12b). The early freeze-back onset at 52 cm at the center, as marked in Figure 13b, was still notable.

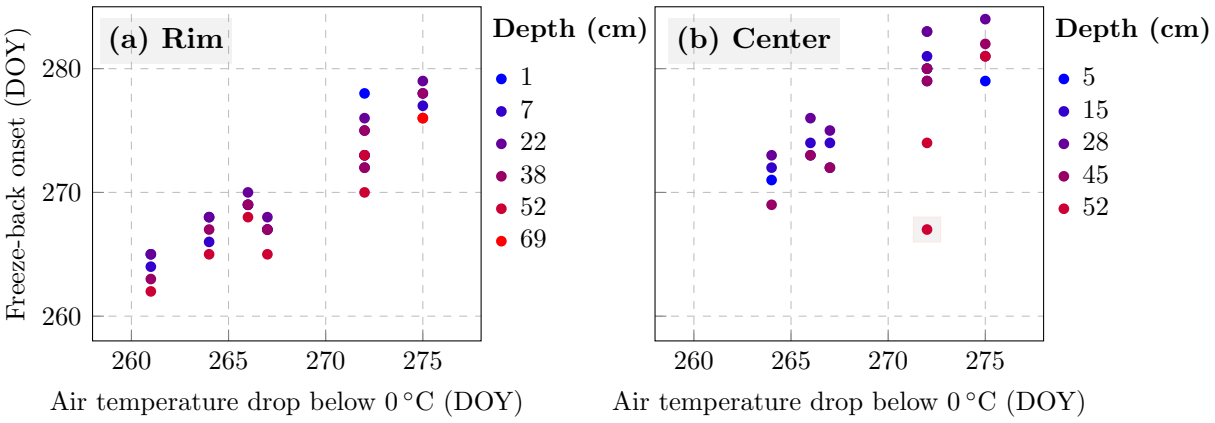

Figure 13: Freeze-back onset depending on the date when air temperature dropped below 0 °C shown for the respective depths at the polygon rim (a) and center (b). The variables are depicted with the unit "day of the year" (DOY) for the entire time series. The marked data point in (b) represents the freeze-back onset of the freshly degraded permafrost at 52 cm in 2018.

4.3 Duration of freeze-back

Figure 14 shows the calculated duration of freeze-back at the rim and center of the polygon at the respective depths. Detailed results and the calculated absolute and percentage change between the consecutive years are listed in the appendix in Table B2. Frozen conditions were generally reached between early October and the middle of January, with a freeze-back duration of 10 d to 101 d.

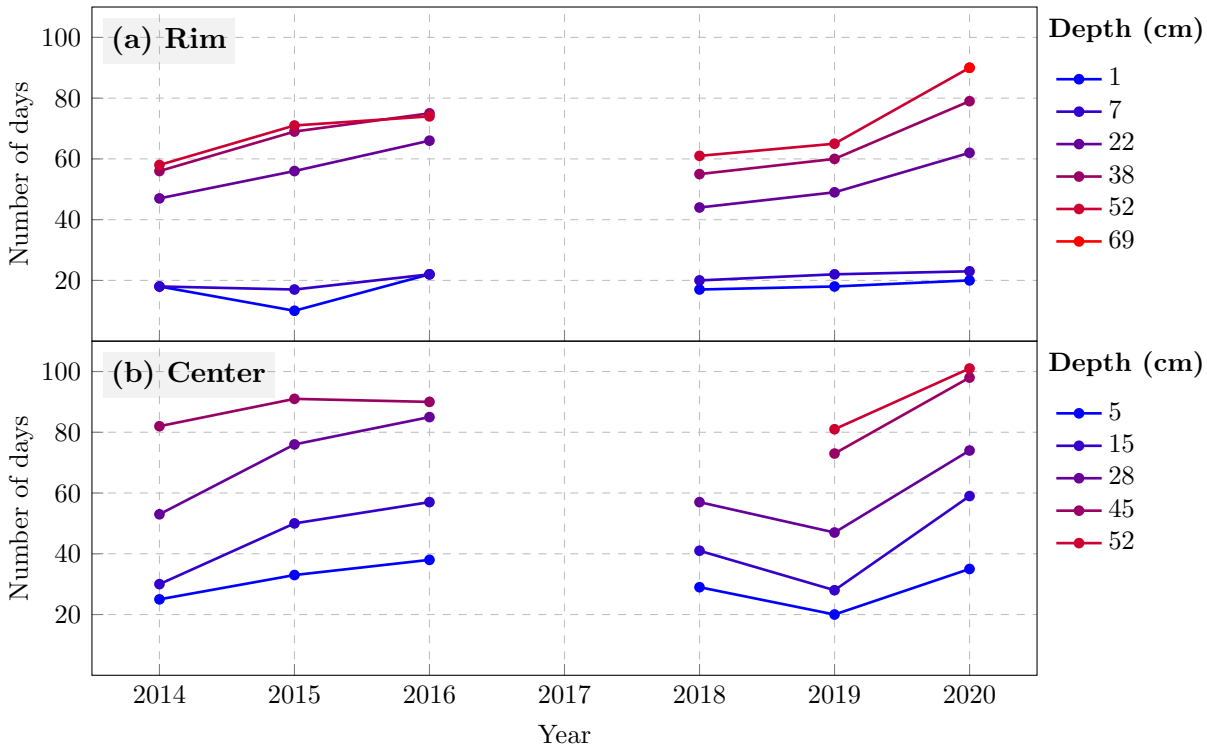

Figure 14: Duration of freeze-back in days at the respective depths at the polygon rim (a) and center (b) during the study period. I calculated the freeze-back duration as described in Section 3.

Rim: At the polygon rim, frozen conditions were reached between early October and early January with a freeze-back duration between 10 d to 90 d, as shown in Figure 14a. Within each respective year, the duration of freeze-back at the polygon rim increased with depth, meaning that shallow depths took less time to refreeze than greater depths. The only exception from this observation occurred in 2016, where the duration at 52 cm was 1 d shorter than at 38 cm. I observed a large difference between the freeze-back duration at 7 cm and at 22 cm. In each year, the duration at 22 cm was more than twice as long as the duration at 7 cm. The absolute difference ranged from 24 d to 44 d. I observed differences between the greater depths as well, although not as big. The difference between 22 cm and 38 cm was 9 d to 17 d, while the difference between 38 cm and 52 cm was only 5 d to 11 d. Furthermore, the freeze-back duration showed inter-annual variability throughout the study period. Unfortunately, no results were available for 2017. During the study period, the freeze-back duration in 2015, but particularly in 2016 and 2020, was much

longer compared to the other years. While the duration at 1 cm and at 7 cm appeared to be relatively stable, greater depths showed a much longer freeze-back duration in these years. The duration ranged between 10 d to 71 d in 2015, 22 d to 75 d in 2016, and 20 d to 90 d in 2020. This was much longer than the freeze-back duration that I observed in the other years (18 d to 58 d in 2014, 17 d to 61 d in 2018, and 18 d to 65 d in 2019). Additionally, 2020 was the first year to include a value for the freeze-back duration at 69 cm, which was 90 d long and thus, along with the duration at 52 cm in that year, the longest freeze-back duration observed within the time series at the polygon rim.

Considering the development from 2014 to 2020, I observed a high inter-annual variability, especially at depths below 7 cm. In particular the years 2015, 2016, and 2020 were noticeable.

Center: Frozen conditions at the polygon center were reached between early October and the middle of January with a freeze-back duration between 20 d to 101 d (Figure 14b). Similar to the rim, the freeze-back duration at the center of the polygon increased with depth within each respective year. I observed generally larger differences between the measured depths at the center than at the rim. However, these differences were not as notable as the large difference observed between 7 cm and 22 cm at the rim. The absolute difference of the freeze-back duration within the time series ranged from 5 d to 24 d between 5 cm and 15 cm, 15 d to 28 d between 15 cm and 28 cm, 5 d to 29 d between 28 cm and 45 cm, and 3 d to 8 d between 45 cm and 52 cm. Freeze-back at the polygon center generally took longer than at the polygon rim. The duration of freeze-back at the polygon center showed great inter-annual variability. Similar to the rim, the years 2015, 2016, and 2020 showed a notably high freeze-back duration within the study period. Opposing to the rim, this was also true for the shallow layers between 5 cm to 15 cm. The duration in these years ranged between 33 d to 91 d in 2015, 38 d to 90 d in 2016, and 35 d to 101 d in 2020. These ranges were much larger than the duration I observed in the other years (25 d to 82 d in 2014, 29 d to 57 d in 2018, and 20 d to 81 d in 2019). Furthermore, 2019 and 2020 included values for the freeze-back duration at 52 cm at the polygon center.

This value was 81 d in 2019 and 101 d in 2020 which was the longest duration within the time series,.

In conclusion, both the rim and the center of the polygon showed great inter-annual variability from 2014 to 2020. At both sites, a notably high freeze-back duration occurred in 2015, 2016, and 2020. This was true for all depths at the polygon center and for depths below 7 cm at the rim. Shallow depths took less time to refreeze than greater depths and the freeze-back duration at the polygon center was longer than at the rim. Due to the large inter-annual variability, the results do not display a distinct increase or trend in the freeze-back duration.

Influence of snow cover: The impact of the start of snow accumulation on the freeze-back duration was another question to consider. Figure 15 shows scatter plots of the start of snow accumulation and the freeze-back duration at the polygon rim and center. At both sites, I did not detect a clear relation between the two variables. It appears that, despite the changing onset of snow accumulation, shallow depths generally showed a short, and greater depths showed a longer zero-curtain period, as shown in Figure 14.

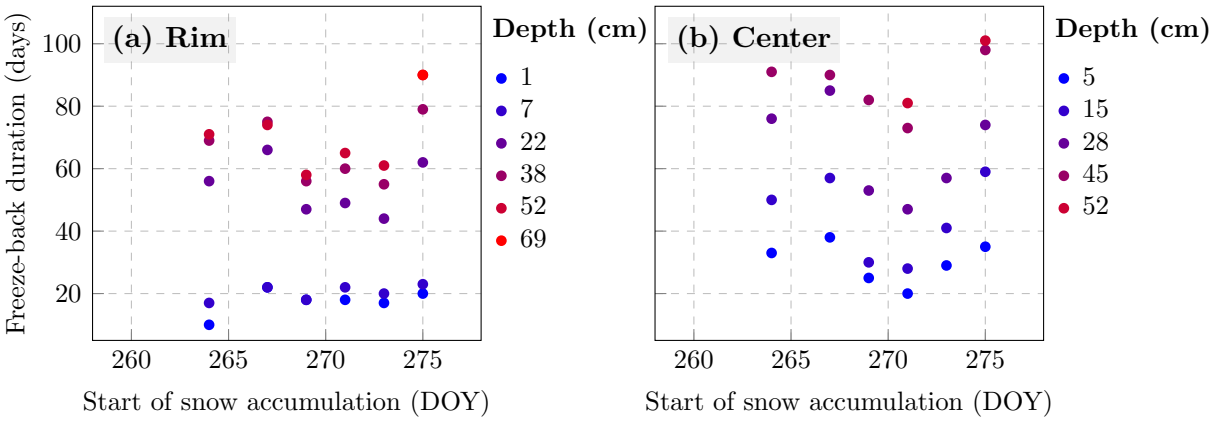

Figure 15: Freeze-back duration depending on the start of snow accumulation at the respective depths at the polygon rim (a) and center (b).

I observed similar results by investigating the relation between the freeze-back duration and decreasing air temperature (Figure 16). At both the polygon rim and center, the freeze-back duration did not seem to be influenced by the air temperature dropping below

0 °C. This indicates that the freeze-back duration was generally influenced by factors other than the onset of snow and decreasing air temperature.

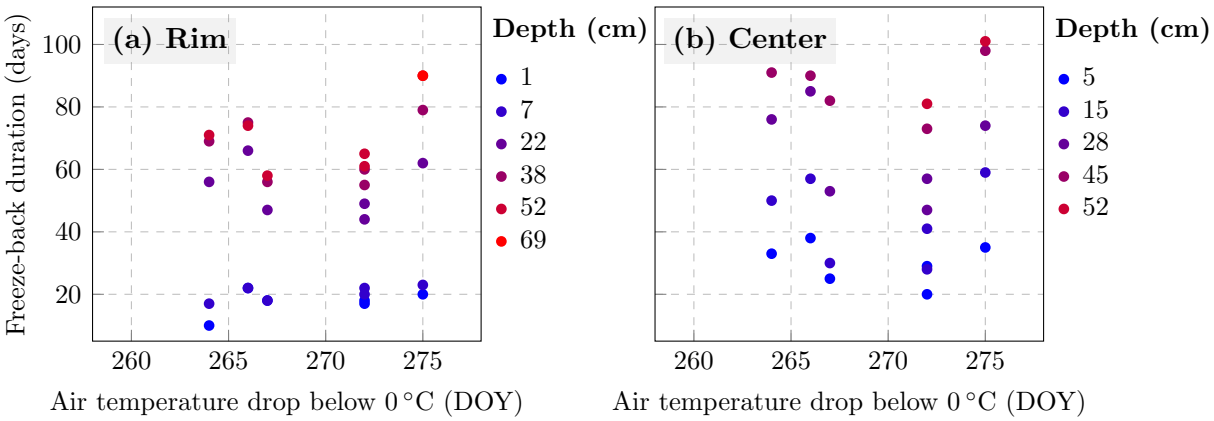

Figure 16: Freeze-back duration depending on the date when air temperature dropped below 0 °C at the respective depths at the polygon rim (a) and center (b).

5 Discussion

The following section contains the discussion of my analysis. First, I discuss the methods that I applied in this work. During the interpretation of my results, I came across some uncertainties produced by my approach. Subsequently, I discuss the results of the active layer freeze-back with respect to its possible drivers as well as previous observations and results obtained in other studies.

5.1 Methodological uncertainties

First, the estimation of the time of start and end of freeze-back was sometimes problematic and caused difficulties for calculating the freeze-back duration. An overview of the start and end of freezing is shown in the appendix in Figure B1. Occasionally, the deepest depths at both the polygon rim and center (69 cm and 52 cm) contained a date for the end of freeze-back, but not for the start of freeze-back. This could either be caused by large gaps in the soil temperature data or by the threshold created for the soil conditions in Section 3. I defined the start of freeze-back as a temperature drop to 0.1 °C followed

by the soil temperature staying within zero-curtain conditions, and the end of freeze-back as the point in time that was followed by at least 10 d of consecutively cold conditions. During active layer warming, the temperature at these great depths increased, but stayed within the zero-curtain threshold, hence never increased to more than 0.1 °C. Therefore, I could not observe a temperature drop to 0.1 °C in fall and did not determine a date for the start of freeze-back. Nevertheless, I did calculate the date for the end of freeze-back, as the temperature dropped below the zero-curtain threshold again. For these depths I could not determine the freeze-back duration. The thresholds that I defined in Section 3 were based on the observed soil temperature at the study site and are therefore most likely not reproducible for different sites. Furthermore, large data gaps (Figure 6) limited the reliability of the results.

Second, an appropriate assessment of the start of snow accumulation was challenging since I retrieved the data from webcam images. For the estimation of the percentage of snow cover and the start of snow accumulation, I considered the entire coverage of the webcam image and not just the polygon. In some years, the autumn snow cover was very patchy at first. In these cases, the polygon was only partly covered by snow. Additionally, wind redistribution caused variable snow depth across the landscape. The variable snow cover and snow depth may have affected the thermal response of the soil differently at the polygon rim and center. Furthermore, I determined the start of snow accumulation as the point in time after which the site stayed snow-covered to some extent, meaning that no snow-free conditions occurred until spring. This means that the snow cover could have been less than 100 % and very thin and patchy. Defining the start of snow cover build-up as the day when the surface is 100 % snow-covered might have produced more reliable results. However, this alternative also would not include information on the snow cover thickness, which could still be very variable and differ between the polygon rim and center. The temporal difference between the start of snow accumulation and the development of a full snow coverage varied between the years. I chose the explained approach in order to include the potential influence of a new and still accumulating snow cover on the freeze-back process. For more reliable results it could have been useful to i) consider only the

polygon with a separate assessment of the rim and center, ii) apply a different definition of the start of snow cover accumulation, and iii) additionally take data on the snow depth into account to obtain information on the spatially and temporally variable snow depth during snow cover accumulation.

Third, the comparison of the polygon rim and center was complicated due to the different observation depths. The soil temperature sensors' depths were measured relative to the surface of the polygon, meaning that for example 52 cm at the polygon rim is horizontally not at the same depth as 52 cm at the polygon center. The vertical exchange processes below the land surface are modulated by the soil's microtopography. Since the sensors at the polygon rim and center were not installed at the exact same depths relative to the surface (except for the sensors at 52 cm), it was challenging to make precise comparisons for these processes between the different depths at the polygon rim and center. It was better to consider them separately and only make comparisons between shallow, intermediate, and deep depths at the rim and center, respectively.

Finally, I estimated the soil condition based on the soil temperature only. I did not consider the soil's volumetric water content which is an important factor in the active layer of permafrost. Including data on the VWC could have been helpful for the analysis and might have produced more reliable results. However, VWC data were not available for the same depths as the soil temperature data, which limited the comparability. Data on VWC were very limited and only available for a fraction of the depths and the time series, which is why I decided to compute the analysis based on mainly the soil temperature.

For the following part of the discussion, I also considered the soil station's VWC and snow depth data which I analysed visually to further discuss my results.

5.2 Soil temperature profile in 2016

I chose 2016 to get a detailed look at the temperature profiles because it had the least missing values out of the time series. Due to the great inter-annual variability within the relatively short time series, it was challenging to classify this year as an average, warm, or cold year. Considering the soil temperature profile at the different depths described in

Section 4, 2016 was not an exceptional year and may have been representative of average conditions in the time series. During the freeze-back period of 2016, the air temperature was slightly warmer than in the previous years. In addition, this year experienced a relatively high snow depth at the beginning of winter (Boike et al., 2022) and a slightly later freeze-back onset and longer duration than the previous year. The bidirectional freezing that I observed in 2016 (Figure 9) occurred throughout the study period. This means that freezing at the polygon rim and center occurred from both the top and the bottom of the active layer, which has been observed in various studies (Osterkamp and Romanovsky, 1997; Boike et al., 1998; Luo et al., 2014; Yi et al., 2019).

The absolute soil temperature varied between the polygon rim and center. Especially in January, February, and December, the soil at all depths at the polygon center was much warmer than at the rim. This was due to the reasonably longer zero-curtain period, influenced by a higher volumetric water content. Latent heat, released during the phase change of water to ice, warms the soil and therefore prevents the soil temperature from decreasing (Gold and Lachenbruch, 1973; Outcalt et al., 1990; Romanovsky and Osterkamp, 2000). Polygon rims are often drier than the centers (Langer et al., 2011a). The maximum VWC at the soil station averaged to approximately 70 % at the rim and 90 % at the center, which explains the observed soil temperature differences.

5.3 Onset of freeze-back

Freeze-back onset can, among other factors, be influenced by air temperature, soil VWC, and snow cover (e.g. Yi et al., 2019). Between 2014 and 2020, my results showed an overall shift towards a later freeze-back onset at both the polygon rim and center. Freeze-back onset between the different depths was relatively stable, which was also observed by Boike et al. (1998) in northern Siberia. The onset generally occurred later at the polygon center compared to the rim.

Since snow delays the thermal response of soil temperature to changes in air temperature (Stieglitz et al., 2003; Park et al., 2015; Vincent et al., 2017), it is expected to influence the onset of active layer freeze-back. This influence has been observed by Yi

et al. (2019), who found an early start of snow accumulation to result in a later start of active layer freeze-back. They observed this influence to be especially strong at shallow depths and weaker at greater depths, which were related to the maximum active layer thickness.

These findings cannot be well represented by my results. While Yi et al. (2019) found a negative relation between the start of snow accumulation and freeze-back onset, I observed a positive relation between these parameters at the polygon rim and center (see Figure 12). It is possible that the influence of snow was of higher magnitude at the polygon center, since the snow can be redistributed by wind, leading to a snow-filled center and exposed rim (Boike et al., 2013). However, I did not observe this influence. Throughout the study period, excluding 2017, a late start of snow accumulation coincided with a late freeze-back onset and vice versa. This positive relation occurred at both the polygon rim and center, with some variability. However, this does not imply a causal connection. As shown in Figure 13, a stronger positive relation existed between the decreasing air temperature and the freeze-back onset. An early or late decreasing air temperature below 0 °C could have resulted in both, a corresponding early or late freeze-back onset and a corresponding early or late start of snow accumulation. Furthermore, the snow cover that established at the start of snow accumulation was usually very thin and therefore did not have a strong insulating effect on the soil temperature. Only the results for 2017 at the polygon rim (since results for 2017 were not available at the center) are in line with the findings of Yi et al. (2019). In 2017, a relatively late start of snow accumulation coincided with early freeze-back onset (Figure 10a, Figure 12a). Nevertheless, this early freeze-back onset could have also been caused by an early decrease in air temperature. As shown in Figure 11, the air temperature drop below 0 °C in 2017 occurred sooner than in the other years. 2017 also showed a larger temporal offset between the decreasing air temperature and the start of snow accumulation. This allowed for the ground to cool much faster and could explain the early freeze-back onset in 2017. I suggest that, for the majority of the time series, air temperature was a stronger driver of the freeze-back onset than snow accumulation.

The soil's volumetric water content plays an important role in the freezing dynamics and could be an explanation for the temporal offset between freeze-back onset at the polygon rim and center. As mentioned above, polygon centers on Samoylov Island are often wet or water-saturated, while the rims are drier (Langer et al., 2011a). VWC data at the soil station indicated a maximum VWC of approximately 50 % to 70 % between different depths at the rim and 70 % to 90 % at the center throughout the study period. The higher VWC at the polygon center resulted in a higher heat capacity, which could have slowed the cooling process. Romanovsky and Osterkamp (2000) observed a generally slowed soil cooling due to the presence of liquid water. Soil temperature sensors were installed at and below 5 cm depth at the center. It is therefore possible that the wet soil above 5 cm cooled slowly and delayed the freeze-back onset at greater depths. Due to topographic differences, the rim possibly cooled faster than the center, which promoted an earlier freeze-back onset at the rim. Moreover, the VWC varied between the different depths. Especially at the rim, VWC was often highest at intermediate depths, followed by shallow depths and the greatest depths. This could also have been a factor determining the variability of the freeze-back onset at the different depths within the soil, as the VWC and the resulting processes showed great variability within a soil profile, which was also observed by Zhao et al. (2022).

5.4 Duration of freeze-back

The duration of the active-layer freeze-back during the study period showed great variability, both between the respective years and depths. This is in line with Boike et al. (1998), who observed a highly variable freeze-back duration in northern Siberia. At Samoylov Island, especially the years 2015, 2016, and 2020 showed a notably long freeze-back duration. Overall, the duration of zero-curtain period was longer at the polygon center compared to the rim.

As shown in Figure 15 and Figure 16, no distinct relation existed between i) the start of snow accumulation and freeze-back duration, and ii) the time of air temperature drop below 0 °C and freezing duration. Opposing to the freeze-back onset, the variability of

the zero-curtain duration seemed to be majorly driven by different factors.

Yi et al. (2019) found an early snow accumulation to result in a longer zero-curtain period and a late accumulation to result in a shorter duration. However, I did not observe such a relation at the study site. It is more likely that the freeze-back duration at Samoylov Island was influenced by snow depth than by the start of snow accumulation. A deeper snow depth can enhance the snow's insulating effect and promote soil warming (Park et al., 2015) and therefore influence the freeze-back duration. Generally, snow depth varies between the polygonal rim and center. Due to the redistribution by wind, snow depth is often much higher at the polygonal centers (Boike et al., 2013; Yi et al., 2014). Martin (2022) investigated the snow depth distribution at a snow station on Samoylov Island. The snow station was located in close proximity to the soil station. From 2014 to 2020, the average maximum snow depth was deepest at the center and shallowest at the rim of the polygon. The maximum snow depth averaged to approximately 61 cm at the center and 44 cm at the rim. The highest values at the rim and center were observed in 2016 and 2017 (Martin, 2022). Due missing results for the freeze-back duration in 2017, this year is negligible for this discussion. The mean maximum snow depth in 2016, as calculated by Martin (2022), was 53 cm at the rim and 71 cm at the center of the polygon. Although these measurements were conducted at a different polygon, a similar snow depth distribution could be expected at the soil station. This distribution resulted in a stronger insulating effect and thus longer freeze-back duration at the center compared to the polygon rim. Moreover, this insulating effect could have been further amplified by latent heat release due to a higher VWC, as described by Goodrich (1982); Romanovsky and Osterkamp (2000), and thus increased the freeze-back duration even more. This could have influenced both the polygon rim and center, but I expect the effect to be of higher magnitude at the center due to its higher VWC. In addition to that, the very long zero-curtain period observed at both the rim, but especially at the polygon center in 2015, 2016, and 2020 may be a result of the strong snowfall events that took place in the respective years as observed at the long-term observatory on Samoylov (Boike et al., 2022). Snow depth was also measured at the soil station, though not distinguished

between the polygon rim and center. In the freezing period, these data showed maximum snow depths of roughly 50 cm in 2014, 55 cm in 2015, up to 80 cm in 2016, 45 cm in 2018 and 2019, and 75 cm in 2020. Data for 2017 were missing. The snow depth in 2015, but especially in 2016 and 2020 was very deep. My observations for 2015 and 2016 were similar to Martin (2022). This deep snow depth could have caused a stronger insulating effect, which possibly extended the freeze-back duration in these years.

However, freeze-back duration is not only influenced by the snow depth. Other properties such as the structure and density, and snow-water equivalent (SWE) of the snow cover play a key role for determining its influence on the ground temperature and zero-curtain (Goodrich, 1982; Zhang et al., 1997; Stieglitz et al., 2003). Snow can hold different amounts of water. SWE refers to the amount of water contained in a given volume of snow (Callaghan et al., 2011) and can have various effects on permafrost. A higher SWE can increase the insulating properties of snow. SWE can act as a thermal buffer, slow the cooling process and therefore impact the freeze-back duration. Freezing SWE in snow releases latent heat, warms the ground temperature, and slows freezing. In the case of snowmelt, SWE contributes to the soil's VWC. Martin (2022) calculated the mean SWE at the end of the snow season (defined as 15 April to 15 May) from 2016 to 2019. The highest SWE was observed in 2016 (148 mm), which could have interacted with the high snow depth observed at the snow station by Martin (2022) and at the soil station. This could have amplified the insulating effect, thus further increasing the freeze-back duration.

Freeze-back duration is closely related to the VWC in the refreezing soil (Luo et al., 2014). In moist soils, the release of latent heat warms the soil significantly through non-conductive heat processes (Outcalt et al., 1990; Zhao et al., 2022). The magnitude of this effect depends on the VWC, i.e. a wet active layer generally shows a more pronounced zero-curtain effect than a dry active layer (Outcalt et al., 1990; Boike et al., 1998). Since the heating effect induced by liquid water during phase change varies greatly for the different depths (Zhao et al., 2022), the soil's VWC could also explain the observed large difference of freeze-back duration between the intermediate depths at the polygon rim. As mentioned above, VWC data at the soil station showed a large variability between the

different depths at the polygon rim. Throughout the study period, VWC at intermediate depths was often higher than at shallow or great depths. During the zero-curtain period, VWC at the shallowest depth (9 cm) decreased much faster than at intermediate depths (24 cm, 38 cm, and 52 cm). This could explain the detected large difference of the freeze-back duration between 7 cm to 22 cm at the rim. Furthermore, this effect explains why the freeze-back duration at the polygon center of the study site generally took longer than the rim (Figure 14), because the low polygon centers had a higher VWC (also observed by e.g. Yi et al., 2014). The soil's VWC in autumn was highly variable and depended on factors such as soil structure, rain events, and evapotranspiration, which was also a possible cause for the variable freeze-back duration. The magnitude of ground warming induced by latent heat release can increase when an insulating snow cover is present (Goodrich, 1982). My results show that greater depths had a longer freeze-back duration than shallow depths, both at the polygon rim and center. This could have generally resulted from insulation at the surface. Slow freezing at shallow depths could have caused a smaller temperature gradient, which caused even slower freezing at greater depths.

The future influence of snow cover on the freezing dynamics of the active layer in Arctic permafrost is coupled to its changes due to the projected warming and increase of precipitation in climate scenarios (Yi et al., 2019; Constable et al., 2022). Depending on those changes, the impact of climate warming on permafrost temperatures and thus freezing dynamics can either be mitigated or intensified by snow cover (Stieglitz et al., 2003). Fall and early winters are affected the most by the Arctic amplification, and this season is crucial for the thermal state of the soil. Especially the snow cover development is uncertain and varies among different regions (Stieglitz et al., 2003; Callaghan et al., 2011; Constable et al., 2022). In recent years, a declining snow cover extent and duration has been observed (Constable et al., 2022). This development is likely to enhance in the future, with a higher percentage of rainfall as precipitation and furthermore a higher SWE in the Arctic (Callaghan et al., 2011; Constable et al., 2022).

6 Summary and conclusion

As a global climate regulator, the Arctic is experiencing manifold climate change impacts, including permafrost thaw. Permafrost degradation poses great ecological, social, and economic risks for the Arctic and the entire globe. A deepening of the active layer can harm Arctic infrastructures and lead to the release of additional greenhouse gases into the atmosphere. Therefore, it is important to investigate the active layer thawing and freezing dynamics in order to assess the risk induced by permafrost thaw. These processes can be influenced by different drivers and vary depending on a region's climatic conditions and topography. Since the Arctic amplification is more strongly pronounced during the freezing period, active layer freezing processes may be particularly sensitive to climate impacts.

This work's objective was to investigate the onset and duration of the active layer freeze-back process at a polygonal tundra site at Samoylov Island in northeastern Siberia. I analyzed soil temperature data from 2014 to 2020 with respect to the polygon's micro-topography. Based on thresholds adjusted to fit the soil temperature data at this site, I estimated the onset and duration of freeze-back at different depths at the elevated polygon rim and topographically lower center, respectively. I determined the start and end of freeze-back for the respective depths and years and calculated the duration of freeze-back. Subsequently, I calculated the absolute (and percentage) change of the freeze-back onset and duration for the study period. Based on webcam images of the study site, I estimated the start of snow accumulation for each year and investigated its influence on the freeze-back process.

From 2014 to 2020, the freeze-back started between the middle of September and the middle of October and ended between early October and the middle of January. The freeze-back duration varied between 10 d to 101 d in different years and depths. Freeze-back generally started later and took longer at the polygon center than at the rim. At both, the polygon rim and center, the start of freeze-back at the different depths was relatively stable and only varied by a few days, whereas the freeze-back duration showed

greater variability between the different depths. Greater depths generally took more time to refreeze than shallow depths. During the study period, the freeze-back onset was shifted towards a later start by 7 d to 11 d. The freeze-back duration showed great inter-annual variability, with notably high values in 2015, but particularly in 2016 and 2020. Towards the end of the study period, active layer thickness at the polygon rim and center increased.

At both, the polygon rim and center, the start of snow accumulation did not have a distinct impact, neither on the freeze-back onset nor on the duration. Freeze-back onset was more closely connected to the air temperature and the contained VWC before freeze-back, the latter being particularly important at the water-saturated polygon center. Early or late air temperature decrease positively affected the onset of freeze-back, while a higher VWC may have prevented fast soil cooling and therefore delayed the start of freeze-back. Meanwhile, the polygon rim cooled faster due to topographic differences.

Freeze-back duration was further influenced by drivers such as snow depth, snow water equivalent, and volumetric water content. A deep snow cover insulated the soil and prevented the ground from cooling. Large amounts of snowfall in 2015, but especially in 2016 and 2020 could have been a major driver of freeze-back duration in these years. This insulating effect could be amplified by a higher SWE. The latent heat release induced by freezing of the soil's VWC further prevented ground freezing. Due to differences in snow distribution, the effect of snow depth and SWE on the freeze-back duration was possibly of higher magnitude at the polygon center. Meanwhile, VWC had a great impact on freeze-back duration at the center but also influenced the duration at intermediate depths at the polygon rim.

In conclusion, the active layer freeze-back process showed great inter-annual variability throughout the study period and behaved differently at the polygon rim and center. The drivers of this process varied and were closely connected to the climatic conditions and the surface's microtopography. The observed later freeze-back onset in combination with a sometimes very long freeze-back duration resulted in an overall longer thawed period. A longer thawed period combined with a deepening active layer implicates the possibility of further carbon decomposition and the release of additional greenhouse gases into the

atmosphere. This, in turn, enhances the permafrost-carbon feedback.

This work highlights the importance of gaining a better understanding of freeze processes and their various driving factors in order to appropriately assess active layer conditions. It is hereby crucial to take the soil's topography into account. The next step could be to integrate data on the VWC in the analysis to determine its influence on the freeze-back process. Further research should investigate the spatial heterogeneity of snow cover accumulation in order to assess its influence on soils with different topographic characteristics. The spatial distribution of snow depth as well as the SWE should also be examined to provide a more precise evaluation of the snow's insulating effect. Furthermore, developing a more reproducible script could be useful to enable analyses at different sites.

For future research at Samoylov Island, it could be interesting to analyze the complete freeze and thaw cycles within the time series in order to gain a more sophisticated understanding of the changing active layer conditions. This could provide valuable information on the changing ratio of thawed and frozen periods which is likely beneficial for assessing past and projecting future greenhouse gas fluxes.

Symbols and abbreviations

T_s Soil temperature (°C)

T_{air} Air temperature (°C)

d day(s)

DOY Day of the year

LTO Long-term observatory

SWE Snow water equivalent (mm)

TDR Time-domain reflectometer

UTC Coordinated universal time

VWC Volumetric water content (%)

Acknowledgements

I want to thank my supervisors Prof. Dr. Julia Boike and Dr. Inge Grünberg for supporting this thesis and for their guidance, expertise, feedback, and valuable input throughout the process. A special thanks to Inge Grünberg for patiently helping me with Python and LaTeX. I want to thank the entire SPARC working group and my fellow students for their support, in particular Benjamin Banaskiewicz, Jennika Hammar, Marie Rolf, Jannika Gottuk, and Luisa Näke for their valuable advice and encouragement.

Bibliography

AMAP: AMAP Arctic Climate Change Update 2021: Key Trends and Impacts, vol. viii+, p. 148pp, Arctic Monitoring and Assessment Programme (AMAP), Tromsø, Norway, 2021.

Biskaborn, B. K., Smith, S. L., Noetzli, J., Matthes, H., Vieira, G., Streletskiy, D. A., Schoeneich, P., Romanovsky, V. E., Lewkowicz, A. G., Abramov, A., Allard, M., Boike, J., Cable, W. L., Christiansen, H. H., Delaloye, R., Diekmann, B., Drozdov, D., Etzelmüller, B., Grosse, G., Guglielmin, M., Ingeman-Nielsen, T., Isaksen, K., Ishikawa, M., Johansson, M., Johannsson, H., Joo, A., Kaverin, D., Kholodov, A., Konstantinov, P., Kröger, T., Lambiel, C., Lanckman, J.-P., Luo, D., Malkova, G., Meiklejohn, I., Moskalenko, N., Oliva, M., Phillips, M., Ramos, M., Sannel, A. B. K., Sergeev, D., Seybold, C., Skryabin, P., Vasiliev, A., Wu, Q., Yoshikawa, K., Zheleznyak, M., and Lantuit, H.: Permafrost is warming at a global scale, Nature Communications, 10, 264, https://doi.org/10.1038/s41467-018-08240-4, 2019.

Boike, J., Roth, K., and Overduin, P. P.: Thermal and hydrologic dynamics of the active layer at a continuous permafrost site (Taymyr Peninsula, Siberia), Water Resources Research, 34, 355–363, https://doi.org/10.1029/97WR03498, 1998.

Boike, J., Grüber, M., Langer, M., Piel, K., and Scheritz, M.: Orthomosaic of Samoylov Island, Lena Delta, Siberia, https://doi.org/10.1594/PANGAEA.786073, 2012.

Boike, J., Kattenstroth, B., Abramova, K., Bornemann, N., Chetverova, A., Fedorova, I., Fröb, K., Grigoriev, M., Grüber, M., Kutzbach, L., Langer, M., Minke, M., Muster, S., Piel, K., Pfeiffer, E. M., Stoof, G., Westermann, S., Wischnewski, K., Wille, C., and Hubberten, H. W.: Baseline characteristics of climate, permafrost and land cover from a new permafrost observatory in the Lena River Delta, Siberia (1998-2011), Biogeosciences, 10, 2105–2128, https://doi.org/10.5194/bg-10-2105-2013, 2013.

Boike, J., Nitzbon, J., Anders, K., Grigoriev, M., Bolshiyanov, D., Langer, M., Lange, S., Bornemann, N., Morgenstern, A., Schreiber, P., Wille, C., Chadburn, S., Gouttevin, I., Burke, E., and Kutzbach, L.: A 16-year record (2002–2017) of permafrost, active-layer, and meteorological conditions at the Samoylov Island Arctic permafrost research site, Lena River delta, northern Siberia: an opportunity to validate remote-sensing data and land surface, snow, and permafrost models, Earth Syst. Sci. Data, 11, 261–299, https://doi.org/10.5194/essd-11-261-2019, 2019.

Boike, J., Cable, W. L., Bolshiyanov, D. Y., Bornemann, N., Grigoriev, M. N., Grünberg, I., and Miesner, F.: Continuous measurements in soil and air at the permafrost long-term observatory at Samoylov Station (2002 et seq), https://doi.org/10.1594/PANGAEA.947032, 2022.

Callaghan, T. V., Johansson, M., Brown, R. D., Groisman, P. Y., Labba, N., Radionov, V., Barry, R. G., Bulygina, O. N., Essery, R. L. H., Frolov, D. M., Golubev, V. N., Grenfell, T. C., Petrushina, M. N., Razuvaev, V. N., Robinson, D. A., Romanov, P., Shindell, D., Shmakin, A. B., Sokratov, S. A., Warren, S., and Yang, D.: The Changing Face of Arctic Snow Cover: A Synthesis of Observed and Projected Changes, Ambio, 40, 17–31, https://doi.org/10.1007/s13280-011-0212-y, 2011.

Constable, A., Harper, S., Dawson, J., Holsman, K., Mustonen, T., Piepenburg, D., and Rost, B.: Cross-Chapter Paper 6: Polar Regions, pp. 2319–2368, Cambridge University Press, Cambridge, UK and New York, USA, https://doi.org/10.1017/9781009325844.023.2319, 2022.

de Koven Leffingwell, E.: Ground-Ice Wedges: The Dominant Form of Ground-Ice on the North Coast of Alaska, The Journal of Geology, 23, 635 – 654, 1915.

Duchkov, A.: Characteristics of Permafrost in Siberia, pp. 81–91, https://doi.org/10.1007/1-4020-4471-2_08, 2006.

Gold, L. W. and Lachenbruch, A. H.: Thermal Conditions in Permafrost- a Review of North American Literature, 1, 3–23, second International Conference on Permafrost Thermal Conditions in Permafrost- a Review of North American Literature, 1973.

Goodrich, L. E.: The influence of snow cover on the ground thermal regime, Canadian Geotechnical Journal, 19, 421–432, https://doi.org/10.1139/t82-047, 1982.

Grigoriev, M.: Cryomorphogenesis in the Lena Delta (in Russian), Permafrost Institute Press, p. 176 pp., 1993.

Grigoriev, N. F.: The temperature of permafrost in the Lena delta basin–deposit conditions and properties of the permafrost in Yakutia, Yakutsk, 2, 97–101, 1960.

Hinkel, K., Paetzold, F., Nelson, F., and Bockheim, J.: Patterns of soil temperature and moisture in the active layer and upper permafrost at Barrow, Alaska: 1993–1999, Global and Planetary Change, 29, 293–309, 2001.

Hinkel, K. M., Outcalt, S. I., and Nelson, F. E.: Temperature Variation and Apparent Diffusivity in the Refreezing Actice Layer, Toolik Lake, Alaska, Permafrost and Periglacial Processes, 1, 265–274, https://doi.org/10.1002/ppp.3430010306, temperature Variation and Apparent Diffusivity in the Refreezing Actice Layer, Toolik Lake, Alaska, 1990.

IPCC: Summary for Policymakers, pp. 3–33, Cambridge University Press, Cambridge, UK and New York, NY, USA, 2022.

Janowiak, M., Connelly, W. J., Dante-Wood, K., Domke, G. M., Giardina, C., Kayler, Z., Marcinkowski, K., Ontl, T., Rodriguez-Franco, C., Swanston, C., Woodall, C. W., and Buford, M.: Considering Forest and Grassland Carbon in Land Management, Report, U.S. Department of Agriculture, Forest Service, Washington Office, https://doi.org/10.2737/wo-gtr-95, 2017.

Kitover, D. C., van Balen, R. T., Roche, D. M., Vandenberghe, J., and Renssen, H.: New Estimates of Permafrost Evolution during the Last 21k Years in Eurasia using Numerical Modelling, Permafrost and Periglacial Processes, 24, 286–303, https://doi.org/10.1002/ppp.1787, 2013.

Lachenbruch, A. H.: Mechanics of Thermal Contraction Cracks and Ice-Wedge Polygons in Permafrost, Geological Society of America, https://doi.org/10.1130/SPE70, 1962.

Lachenbruch, A. H.: Contraction theory of ice-wedge polygons: a qualitative discussion., Nat. Acad. Sci., Natl. Res. Counc. Publ., 1287, 63–71, 1963.

Langer, M., Westermann, S., Muster, S., Piel, K., and Boike, J.: The surface energy balance of a polygonal tundra site in northern Siberia – Part 1: Spring to fall, The Cryosphere, 5, 151–171, https://doi.org/10.5194/tc-5-151-2011, 2011a.

Langer, M., Westermann, S., Muster, S., Piel, K., and Boike, J.: The surface energy balance of a polygonal tundra site in northern Siberia – Part 2: Winter, The Cryosphere, 5, 509–524, https://doi.org/10.5194/tc-5-509-2011, 2011b.

Lenton, T. M., Held, H., Kriegler, E., Hall, J. W., Lucht, W., Rahmstorf, S., and Schellnhuber, H. J.: Tipping elements in the Earth's climate system, Proceedings of the National Academy of Sciences, 105, 1786–1793, https://doi.org/10.1073/pnas.0705414105, 2008.

Luo, D., Jin, H., Lü, L., and Wu, Q.: Spatiotemporal characteristics of freezing and thawing of the active layer in the source areas of the Yellow River (SAYR), Chinese Science Bulletin, 59, 3034–3045, https://doi.org/10.1007/s11434-014-0189-6, 2014.

MacKay, J.: Thermally induced movements in ice-wedge polygons, western arctic coast: a long-term study, Géographie physique et Quaternaire, 54, 41–68, https://doi.org/10.7202/004846ar, 2000.

Martin, J.: Influence of the inter-annual variability of snow physical properties on the ground thermal regime - through observations and modelling (Samoylov Island, Siberia), Ph.D. thesis, Department Geoscience, University of Bremen, 2022.

Morgenstern, A., Grosse, G., and Schirrmeister, L.: Genetic, Morphological, and Statistical Characterization of Lakes in the Permafrost-Dominated Lena Delta, in: Permafrost : proceedings of the 9th International Conference on Permafrost, 29 June - 3 July 2008, Fairbanks, Alaska / edited by D.L. Kane, K.M. Hinkel, (eds), Institute of Northern Engineering, University of Alaska Fairbanks, pp. 1239–1244, URL `http://www.nicop.org/`, 2008.

Muster, S., Langer, M., Heim, B., Westermann, S., and Boike, J.: Subpixel heterogeneity of ice-wedge polygonal tundra: a multi-scale analysis of land cover and evapotranspiration in the Lena River Delta, Siberia, Tellus B, 64, https://doi.org/10.3402/tellusb.v64i0.17301, 2012.

NASA Landsat Program: Lena Delta in Landsat 7/ETM+, 2000.

Obu, J.: How Much of the Earth's Surface is Underlain by Permafrost?, Journal of Geophysical Research: Earth Surface, 126, e2021JF006 123, https://doi.org/10.1029/2021JF006123, 2021.

Osterkamp, T. E. and Romanovsky, E. E.: Freezing of the active layer on the coastal plain of the Alaskan Arctic, Permafrost and Periglacial Processes, 8, 23–44, https://doi.org/10.1002/(SICI)1099-1530(199701)8:1⟨23::AID-PPP239⟩3.0.CO;2-2, 1997.

Outcalt, S. I., Nelson, F. E., and Hinkel, K. M.: The zero-curtain effect: Heat and mass transfer across an isothermal region in freezing soil, Water Resources Research, 26, 1509–1516, https://doi.org/10.1029/WR026i007p01509, 1990.

Park, H., Fedorov, A. N., Zheleznyak, M. N., Konstantinov, P. Y., and Walsh, J. E.: Effect of snow cover on pan-Arctic permafrost thermal regimes, Climate Dynamics, 44, 2873–2895, https://doi.org/10.1007/s00382-014-2356-5, 2015.

Park, S.-E., Bartsch, A., Sabel, D., Wagner, W., Naeimi, V., and Yamaguchi, Y.: Monitoring freeze/thaw cycles using ENVISAT ASAR Global Mode, Remote Sensing of Environment, 115, 3457–3467, https://doi.org/10.1016/j.rse.2011.08.009, 2011.

Romanovskii, N.: Formirovanie poligonal'no-zhil'nykh struktur (Formation of polygonal wedge-structures), 1977.

Romanovsky, V. E. and Osterkamp, T. E.: Effects of unfrozen water on heat and mass transport processes in the active layer and permafrost, Permafrost and Periglacial Processes, 11, 219–239, https://doi.org/10.1002/1099-1530(200007/09)11:3⟨219::AID-PPP352⟩3.0.CO;2-7, 2000.

Schaefer, K., Zhang, T., Bruhwiler, L., and Barrett, A.: Amount and Timing of Permafrost Carbon Release in Response to Climate Warming, Tellus B, 63, 165–180, https://doi.org/10.1111/j.1600-0889.2011.00527.x, 2011.

Schuur, E. A. G., McGuire, A. D., Schädel, C., Grosse, G., Harden, J. W., Hayes, D. J., Hugelius, G., Koven, C. D., Kuhry, P., Lawrence, D. M., Natali, S. M., Olefeldt, D., Romanovsky, V. E., Schaefer, K., Turetsky, M. R., Treat, C. C., and Vonk, J. E.: Climate change and the permafrost carbon feedback, Nature, 520, 171–179, https://doi.org/10.1038/nature14338, 2015.

Schwamborn, G., Rachold, V., and Grigoriev, M. N.: Late Quaternary Sedimentation History of the Lena Delta, Quaternary international, 89, 119–134, 2002.

Stieglitz, M., Déry, S. J., Romanovsky, V. E., and Osterkamp, T. E.: The role of snow cover in the warming of arctic permafrost, Geophysical Research Letters, 30, https://doi.org/10.1029/2003GL017337, 2003.

Van Everdingen, R.: Multi-language Glossary of Permafrost and Related Ground-ice Terms, International Permafrost Association (IPA), revised edition 2005 edn., 1998.

Vincent, W. F., Lemay, M., and Allard, M.: Arctic permafrost landscapes in transition: towards an integrated Earth system approach, Arctic Science, 3, 39–64, https://doi.org/10.1139/as-2016-0027, 2017.

Wagner, D., Wille, C., Kobabe, S., and Pfeiffer, E. M.: Simulation of freezing-thawing cycles in a permafrost microcosm for assessing microbial methane production under extreme conditions, Permafrost and Periglacial Processes, 14, 367–374, https://doi.org/10.1002/ppp.468, 2003.

Wetterich, S., Tumskoy, V., Rudaya, N., Andreev, A. A., Opel, T., Meyer, H., Schirrmeister, L., and Hüls, M.: Ice Complex formation in arctic East Siberia during the MIS3 Interstadial, Quaternary Science Reviews, 84, 39–55, https://doi.org/10.1016/j.quascirev.2013.11.009, 2014.

Yi, S., Wischnewski, K., Langer, M., Muster, S., and Boike, J.: Freeze/thaw processes in complex permafrost landscapes of northern Siberia simulated using the TEM ecosystem model: Impact of thermokarst ponds and lakes, Geoscientific Model Development, 7, 1671–1689, https://doi.org/10.5194/gmd-7-1671-2014, 2014.

Yi, Y., Kimball, J. S., Chen, R. H., Moghaddam, M., and Miller, C. E.: Sensitivity of active-layer freezing process to snow cover in Arctic Alaska, Cryosphere, 13, 197–218, https://doi.org/10.5194/tc-13-197-2019, 2019.

Zhang, T., Osterkamp, T. E., and Stamnes, K.: Effects of Climate on the Active Layer and Permafrost on the North Slope of Alaska, U.S.A, Permafrost and Periglacial Processes, 8, 45–67, https://doi.org/10.1002/(SICI)1099-1530(199701)8:1⟨45::AID-PPP240⟩3.0.CO;2-K, 1997.

Zhao, Y., Nan, Z., Ji, H., and Zhao, L.: Convective heat transfer of spring meltwater accelerates active layer phase change in Tibet permafrost areas, Cryosphere, 16, 825–849, https://doi.org/10.5194/tc-16-825-2022, 2022.

Zimov, S. A., Schuur, E. A. G., and Chapin, F. S.: Permafrost and the Global Carbon Budget, Science, 312, 1612–1613, https://doi.org/10.1126/science.1128908, 2006.

Appendix A

Quality flagging system

Table A1: Quality flagging system used for soil temperature data at Samoylov, implemented by Boike et al. (2019).

Flag	Meaning	Description
0	Good data	All quality tests passed
1	No data	Missing value
2	System error	System failure led to corrupted data, e.g. when the power supply broke down, sensors were removed from their proper location, sensors broke or the data logger saved error codes
3	Maintenance	Values influenced by the installation, calibration, and cleaning of sensors or programming of the data logger; information from field protocols of engineers
4	Physical limits	Values outside the physically possible or likely limits, e.g. relative humidity should be in a range of 0-100%
5	Gradient	Values unlikely because of prolonged constant periods or high/low spikes; test within each single series
6	Plausibility	Values unlikely in comparison with other series or for a given time of the year; partly rule-based or flagged manually by engineers
7	Decreased accuracy	Values with decreased sensor accuracy, e.g. identified when thawing
8	Snow covered	Good data, but the sensor is snow covered

Soil temperature data gap treatment

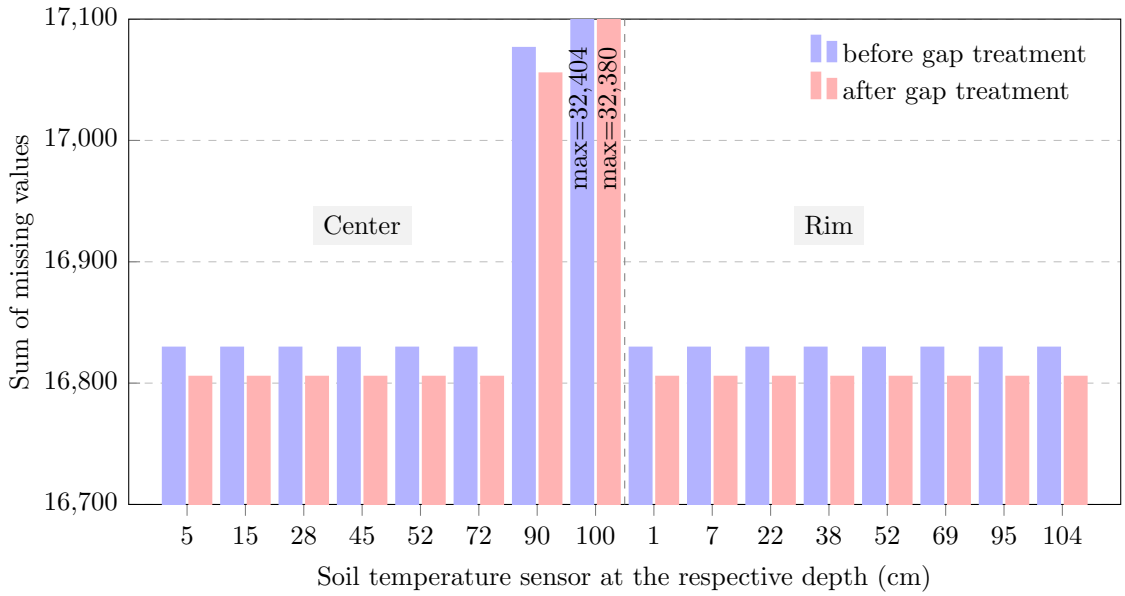

Figure A1: Summary of the missing hourly values for all soil temperature sensors at the polygon rim and center before and after the gap treatment. I was able to reduce he number of missing values for all sensors, yet it was still very high. Especially the sensors at the center at 90 cm and 100 cm had a large number of missing values. The maximum values for those sensors are written on the respective bars, as the values were too high to be included in the plot.

Appendix B

Start and end of freeze-back

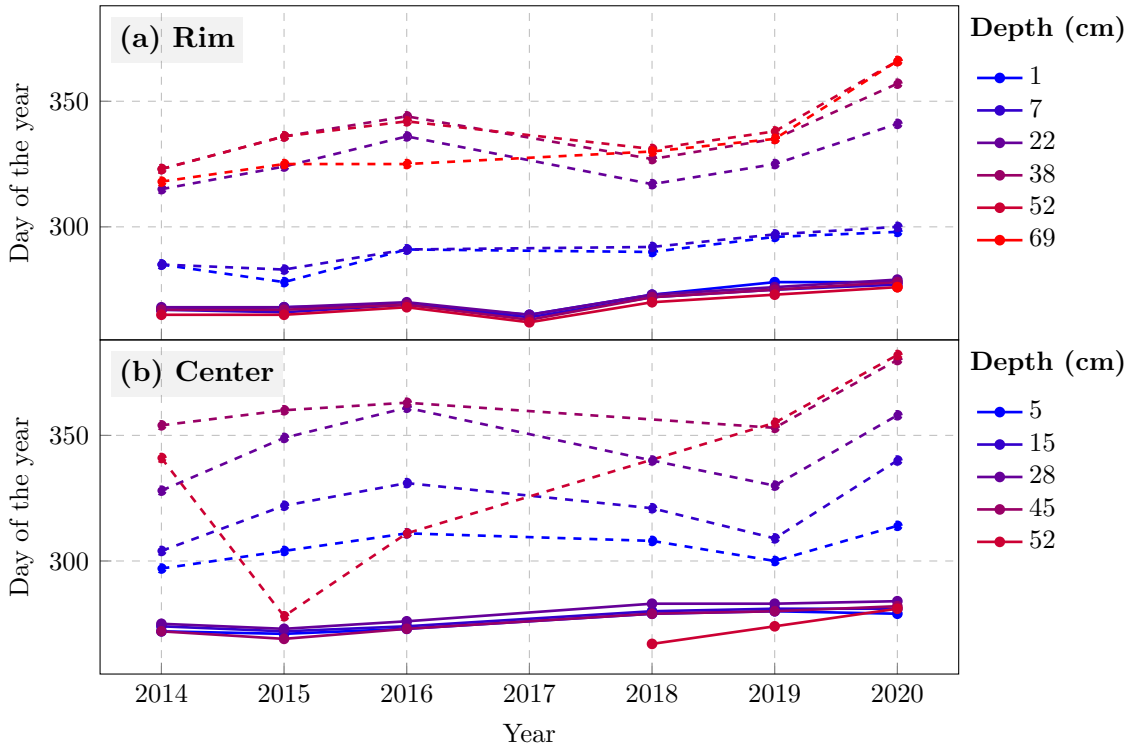

Figure B1: Start (solid) and end (dashed) of freeze-back at the respective depths at the polygon rim (a) and center (b) during the study period.

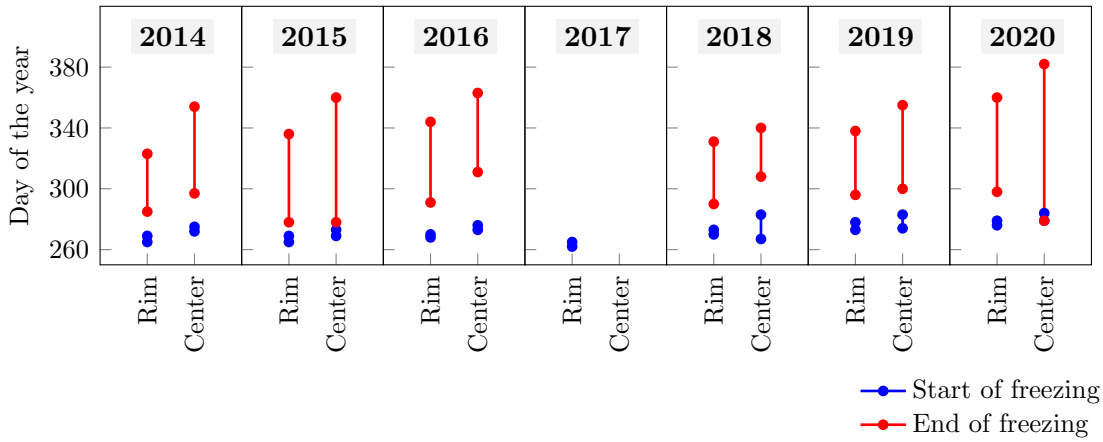

Figure B2: Range of start and end of freezing (minimum and maximum values) at the polygon rim and center for the respective year of the time series. The length of the lines represents the variability with sensor depth. The first 'End of freezing' at the center in 2020 represents the greatest depth which has not been completely thawed in summer.

Onset of freeze-back

Table B1: Freeze-back onset: Results (a, b) as DOY and absolute change in days as compared to the previous year and for the overall period (c, d) at the polygon rim and center, respectively.

Depth (cm)	1	7	22	38	52	69
2014	267	267	268	267	265	
2015	268	266	268	267	265	
2016	269	269	270	269	268	
2017	265	264	265	263	262	
2018	273	272	273	272	270	
2019	278	275	276	275	273	
2020	278	277	279	278	276	276

(a) Freeze-back onset: polygon rim.

Depth (cm)	5	15	28	45	52
2014	272	274	275	272	
2015	271	272	273	269	
2016	273	274	276	273	
2017					
2018	279	280	283	279	267
2019	280	281	283	280	274
2020	279	281	284	282	281

(b) Freeze-back onset: polygon center.

Depth (cm)	1	7	22	38	52
2015	1	−1	0	0	0
2016	1	3	2	2	3
2017	−4	−5	−5	−6	−6
2018	8	8	8	9	8
2019	5	3	3	3	3
2020	0	2	3	3	3
2014 - 2020	11	10	11	11	11

(c) Absolute change of the freeze-back onset at the polygon rim.

Depth (cm)	5	15	28	45	52
2015	−1	−2	−2	−3	
2016	2	2	3	4	
2017					
2018					
2019	1	1	0	1	7
2020	−1	0	1	2	7
2014 - 2020	7	7	9	10	

(d) Absolute change of the freeze-back onset at the polygon center.

Duration of freeze-back

Table B2: Duration of freeze-back: Results (a, b) in days and absolute and percentage change as compared to the previous year and for the overall period (c, d) at the polygon rim and center, respectively.

Depth (cm)	1	7	22	38	52	69
2014	18	18	47	56	58	
2015	10	17	56	69	71	
2016	22	22	66	75	74	
2017						
2018	17	20	44	55	61	
2019	18	22	49	60	65	
2020	20	23	62	79	90	90

(a) Freeze-back duration: polygon rim.

Depth (cm)	5	15	28	45	52
2014	25	30	53	82	
2015	33	50	76	91	
2016	38	57	85	90	
2017					
2018	29	41	57		
2019	20	28	47	73	81
2020	35	59	74	98	101

(b) Freeze-back duration: polygon center.

Depth (cm)	1		7		22		38		52	
Difference	**days**	**%**	**days**	**%**	**days**	**%**	**days**	**%**	**days**	**%**
2015	−8	−44.44	−1	−5.56	9	19.15	13	23.31	13	22.41
2016	12	120.00	5	29.41	10	17.86	6	8.70	3	4.23
2017										
2018										
2019	1	5.88	2	10.00	5	11.36	5	9.09	4	6.56
2020	2	11.11	1	4.55	13	26.53	19	31.67	25	38.46
2014 - 2020	2	11.11	5	27.78	15	31.91	23	41.07	32	55.17

(c) Absolute and percentage change of the freeze-back duration at the polygon rim.

Depth (cm)	5		15		28		45		52	
Difference	**days**	**%**	**days**	**%**	**days**	**%**	**days**	**%**	**days**	**%**
2015	8	32.00	20	66.67	23	43.40	9	10.98		
2016	5	15.15	7	14.00	9	11.84	−1	−1.10		
2017										
2018										
2019	−9	−31.03	−13	−31.71	−10	−17.54				
2020	15	75.00	31	110.71	27	57.45	25	34.25	20	24.69
2014 - 2020	10	40.00	29	96.67	21	39.62	16	19.51		

(d) Absolute and percentage change of the freeze-back duration at the polygon center.

Erklärung

Ich erkläre, dass ich die vorliegende Arbeit oder Teile davon nicht für andere Prüfungs- und Studienleistungen eingereicht, selbständig und nur unter Verwendung der angegebenen Literatur und Hilfsmittel angefertigt habe. Sämtliche fremde Quellen, inklusive Internetquellen, Grafiken, Tabellen und Bilder, die ich unverändert oder abgewandelt wiedergegeben habe, habe ich als solche kenntlich gemacht. Mir ist bekannt, dass Verstöße gegen diese Grundsätze als Täuschungsversuch bzw. Täuschung geahndet werden.

Berlin, den

Maybrit Pia Goldau